

Article

Triterpenoids and Their Glycosides from *Glinus oppositifolius* with Antifungal Activities against *Microsporum Gypseum* and *Trichophyton Rubrum*

Dongdong Zhang ^{1,2} , Yao Fu ^{1,2}, Jun Yang ^{1,2}, Xiao-Nian Li ², Myint Myint San ³,
Thaung Naing Oo ³, Yuehu Wang ^{1,2,*} and Xuefei Yang ^{1,2,*}

¹ Southeast Asia Biodiversity Research Institute, Chinese Academy of Sciences, Yezin, Nay Pyi Taw 05282, Myanmar; zhangdongdong@mail.kib.ac.cn (D.Z.); fuyao@mail.kib.ac.cn (Y.F.); yangjuna@mail.kib.ac.cn (J.Y.)

² Key Laboratory of Economic Plants and Biotechnology and Yunnan Key Laboratory for Wild Plant Resources, State Key Laboratory of Phytochemistry and Plant Resources in West China, Kunming Institute of Botany, Chinese Academy of Sciences, Kunming 650201, China; lixiaonian@mail.kib.ac.cn

³ Forest Research Institute, Yezin, Nay Pyi Taw 05282, Myanmar; dawmyintmyintsanyezin@gmail.com (M.M.S.); tnoo71@gmail.com (T.N.O.)

* Correspondence: wangyuehu@mail.kib.ac.cn (Y.W.); xuefei@mail.kib.ac.cn (X.Y.)

Received: 5 May 2019; Accepted: 7 June 2019; Published: 12 June 2019



Abstract: Four new triterpenoids, 3 β ,12 β ,16 β ,21 β ,22-pentahydroxyhopane (1), 12 β ,16 β ,21 β ,22-tetrahydroxyhopan-3-one (2), 3-oxo-olean-12-ene-28,30-dioic acid (3), and 3 β -hydroxyoleana-11,13(18)-diene-28,30-dioic acid 30-methyl ester (4); 21 new triterpenoid saponins, glinusopposides A–U (5–25); and 12 known compounds (26–37) were isolated from the whole plants of *Glinus oppositifolius*. The structures of the new compounds were elucidated based on the analysis of one-dimensional (1D) and two-dimensional (2D) nuclear magnetic resonance (NMR) and mass spectrometry (MS) data. All compounds from the plants were measured for antifungal activities against *Microsporum gypseum* and *Trichophyton rubrum*. Glinusopposide B (6), glinusopposide Q (21), glinusopposide T (24), and glinusopposide U (25) showed strong inhibitory activities against *M. gypseum* (MIC₅₀ 7.1, 6.7, 6.8, and 11.1 μ M, respectively) and *T. rubrum* (MIC₅₀ 14.3, 13.4, 11.9, and 13.0 μ M, respectively). For those active compounds with an oleanane skeleton, glycosylation (21–26) or oxidation (3) of 3-OH was helpful in increasing the activity; replacement of the 30-methyl group (29) by a carboxymethyl group (26) enhanced the activity; the presence of 11,13(18) double bonds (20) decreased the activity.

Keywords: *Glinus oppositifolius*; triterpenoids and triterpenoid saponins; antifungal activity

1. Introduction

Dermatophytosis is one of the most common skin diseases in animals and humans, which is mainly caused by *Epidermophyton*, *Microsporum* and *Trichophyton* [1,2]. As a chronic disease, dermatophytosis is difficult to treat due to the drug resistance developed by the related fungus [2]. Therefore, it is important to search for novel agents to treat dermatophytosis.

Glinus oppositifolius (L.) Aug. DC. (Syn: *Mollugo spergula* L. and *Mollugo oppositifolia* L; family: Molluginaceae) is a small herb widely distributed in tropical Asia, tropical Africa, and Australia [3]. Traditionally it has been used for treating skin and various infectious diseases in Bangladesh, China, India, Mali and Myanmar [4–6]. As a Chinese folk medicine, the whole plants of *G. oppositifolius* are used to treat diarrhea, coughs, hyperthermia, heat rashes, pinkeye, furuncles, snakebites, and burns [6]. The plant is reputed in Indian medicine due to its antiseptic and antidermatitic properties [7]. It is used to treat leprosy, leukoderma, heart, and skin diseases in the traditional medicine of Myanmar [5].

The major secondary metabolites from *G. oppositifolius* are triterpenoids and their glycosides, which exhibit α -glucosidase inhibitory [8], cytotoxic [9], and antiprotozoal activities [10]. There is little research reported the anti-fungal activities of *G. oppositifolius*. In this study, we isolated 25 new triterpenoids and triterpenoid saponins (Figure 1), along with 12 known compounds in the whole plants of *G. oppositifolius*. Their antifungal properties against *Microsporium gypseum* and *Trichophyton rubrum* were analyzed.

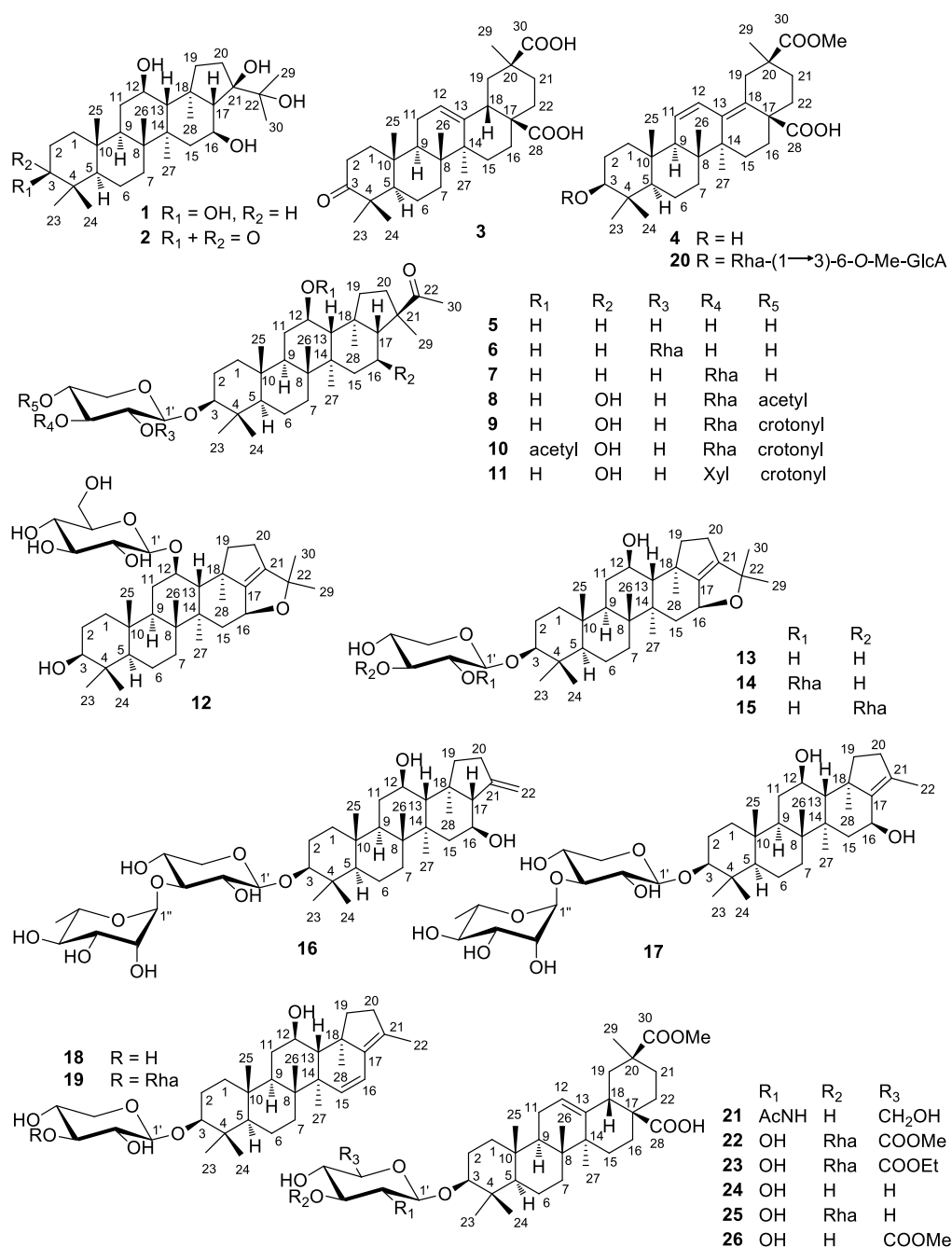


Figure 1. Chemical structures of compounds 1–26 from *Glinus oppositifolius*.

2. Results and Discussion

2.1. Structure Elucidation of the Compounds

Compound 1 had the molecular formula $C_{30}H_{52}O_5$ based on ^{13}C -NMR data (Table 1) and the positive ion at m/z 515.3718 $[M + Na]^+$ (calcd. for $C_{30}H_{52}NaO_5$, 515.3712) in the high resolution

electrospray ionization mass spectroscopy (HRESIMS). The ^1H -NMR spectrum showed resonances for eight methyl groups at δ_{H} 1.61 (s), 1.56 (s), 1.21 (s), 1.19 (s), 1.13 (s), 1.01 (s), 0.97 (s), and 0.82 (s), as well as three oxymethines at δ_{H} 4.48 (m), 4.23 (m), and 3.44 (br t, $J = 8.3$ Hz) (Table 1). The ^{13}C -NMR spectrum showed resonances for thirty carbon atoms as expected from high resolution mass spectrum, which were sorted by DEPT into eight methyls, eight methylenes, seven methines (three oxymethines, δ_{C} 78.0, 69.1, and 66.8), and seven quaternary carbons group, including two oxygenated quaternary carbons. These NMR data were very similar to those of a known hopane triterpenoid saponin from this plant, glinoside C, except for the lack of signals for glucopyranose [8]. The full NMR assignments and connections were determined by ^1H -detected heteronuclear single quantum coherence (HSQC), ^1H -detected heteronuclear multiple bond correlation (HMBC), and ^1H - ^1H correlation spectroscopy (COSY) analyses.

According to the ^1H - ^1H COSY correlations in the 2D spectra of **1** (Figure 2), five connections, C-1-C-2-C-3, C-5-C-6-C-7, C-9-C-11-C-12-C-13, C-15-C-16-C-17, and C-19-C-20, were confirmed. The planar structure of **1** was further deduced as 3,12,16,21,22-pentahydroxyhopane by the HMBC correlations from H_3 -23 and H_3 -24 to C-3, C-4, and C-5; from H_3 -25 to C-1, C-5, C-9, and C-10; from H_3 -26 to C-7, C-9, and C-14; from H_3 -27 to C-8, C-13, and C-15; from H_3 -28 to C-13, C-17, C-18, and C-19; from H_3 -29 and H_3 -30 to C-21 and C-22; and from H-17 to C-19 and C-22. The configurations of 3-OH, 12-OH, 16-OH, and 21-OH were deduced as $3\beta, 12\beta, 16\beta, 21\beta$ by the key nuclear overhauser effect spectroscopy (ROESY) correlations of H-3/H-5, H-5/H-9, H-9/H-12, H-16/ H_3 -27, H-16/ H_3 -28, H-16/ H_3 -30, and H_3 -30/ H_3 -28. Thus, the structure of **1** was determined to be $3\beta, 12\beta, 16\beta, 21\beta, 22$ -pentahydroxyhopane. The absolute configuration was assigned by Cu $K\alpha$ X-ray crystallographic analysis (Figure 3).

Table 1. ^1H (500 MHz) and ^{13}C (126 MHz) NMR data of **1** and **2** in Pyridine- d_5 (δ in ppm, J in Hz).

No.	1		2	
	δ_{H}	δ_{C}	δ_{H}	δ_{C}
1	1.68 m	39.1	1.79 m	39.4
	0.97 m		1.31 m	
2	1.81 m	28.3	2.48 m	34.4
			2.42 m	
3	3.44 br t (8.3)	78.0		216.4
4		39.5		47.4
5	0.78 dd (12.0, 1.7)	55.7	1.28 m	54.8
6	1.51 m	18.9	1.37 m	20.0
	1.33 m		1.31 m	
7	1.43 m	33.6	1.38 m	32.7
	1.21 m		1.19 m	
8		45.1		45.2
9	1.39 m	49.3	1.39 m	48.4
10		37.3		36.8
11	2.11 m	33.2	2.04 m	33.4
	1.64 m		1.65 m	
12	4.23 m	69.1	4.20 m	69.0
13	1.84 d (10.7)	56.4	1.84 d (10.8)	56.5
14		41.8		41.7
15	1.93 dd (12.7, 4.2)	46.0	1.92 dd (12.6, 4.3)	45.9
	1.71 m		1.70 m	
16	4.48 m	66.8	4.48 m	66.7
17	2.41 d (11.7)	73.8	2.41 d (11.6)	73.8
18		47.5		47.5
19	2.60 m	43.1	2.60 m	43.1
	2.14 m		2.13 m	
20	2.05 m	37.8	2.07 m	37.8
	1.95 m		1.96 m	
21		85.7		85.7

Table 1. Cont.

No.	1		2	
	δ_H	δ_C	δ_H	δ_C
22		75.5		75.5
23	1.21 s	28.7	1.11 s	26.6
24	1.01 s	16.3	1.00 s	21.3
25	0.82 s	16.1	0.81 s	15.6
26	0.97 s	17.0	0.95 s	16.6
27	1.13 s	19.5	1.10 s	19.4
28	1.19 s	17.3	1.19 s	17.3
29	1.56 s	26.6	1.56 s	26.7
30	1.61 s	27.3	1.61 s	27.4
3-OH	5.78 br s			
12-OH	5.32 d (6.0)		5.38 d (6.9)	

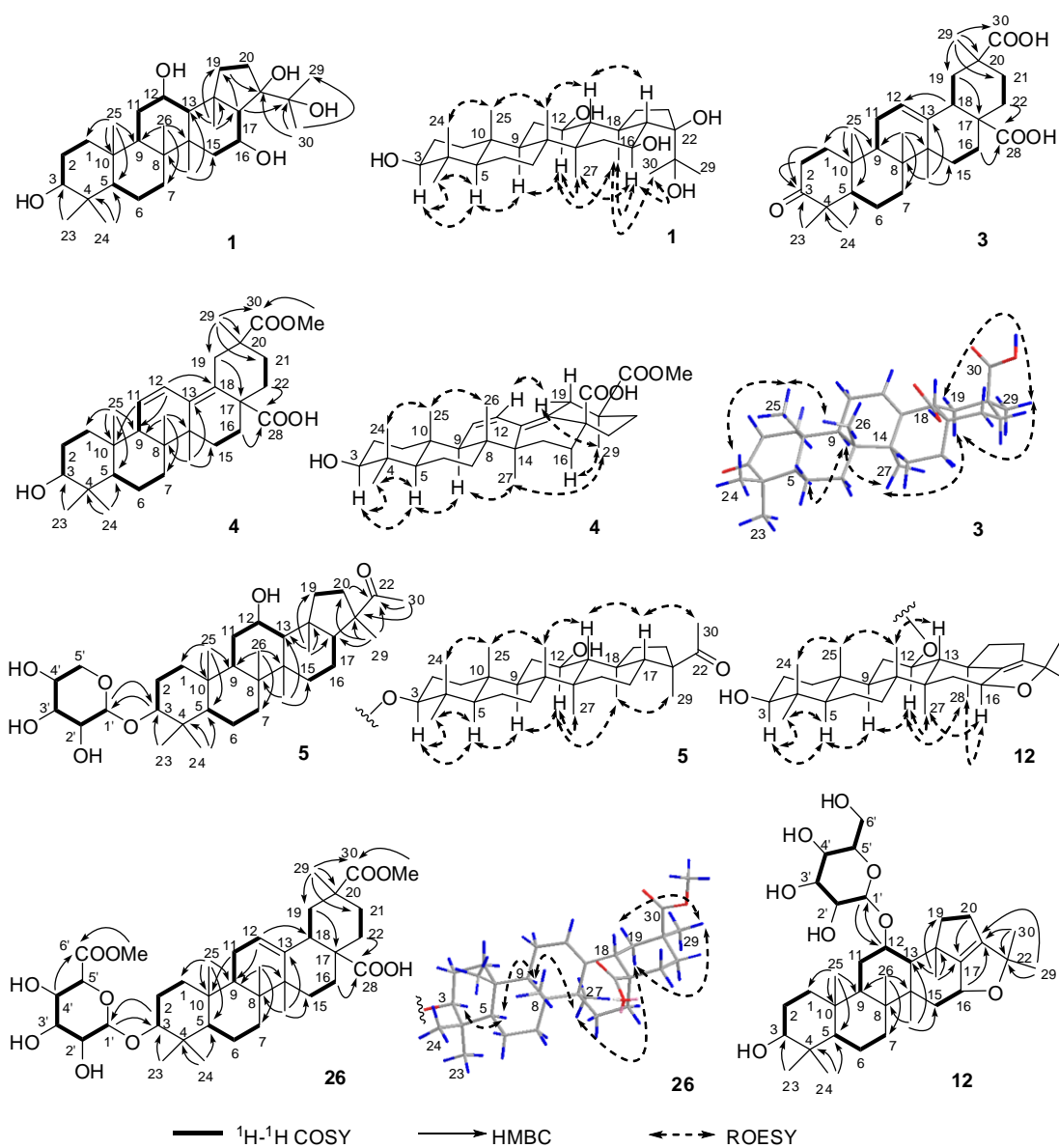


Figure 2. Key 2D-NMR correlations of 1, 3–5, 12, and 26.

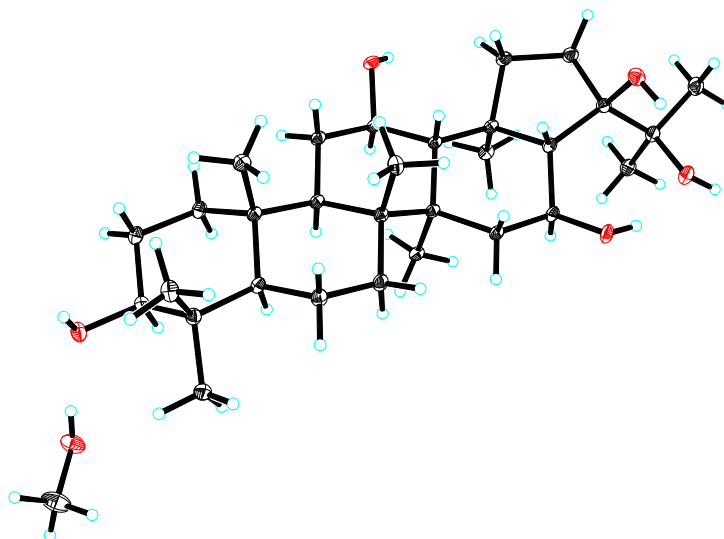


Figure 3. X-ray crystallographic structure of 1.

Compound 2 showed a molecular formula of $C_{30}H_{50}O_5$ based on ^{13}C -NMR data (Table 1) and the $[M + Na]^+$ ion at m/z 513.3551 (calcd. for $C_{30}H_{50}NaO_5$, 513.3556) in the HRESIMS. The NMR data (Table 1) of 2 were analogous to those of 1 except that the signal (δ_C 78.0) for an oxygenated methine in the ^{13}C -NMR spectrum of 1 was replaced by the signal (δ_C 216.4) for a carbonyl group in the ^{13}C -NMR spectrum of 2. The structure of 2 was easily established as 12 β , 16 β , 21 β , 22-tetrahydroxyhopan-3-one by the COSY, HMBC, and ROESY spectra of 2 (Supplementary Materials).

Compound 3 was assigned the molecular formula $C_{30}H_{44}O_5$ based on ^{13}C -NMR data (Table 2) and positive ion mode HRESIMS, which showed a pseudomolecular ion peak at m/z 507.3084 $[M + Na]^+$ (calcd. for $C_{30}H_{44}NaO_5$, 507.3086). The 1H -NMR data of 3 (Table 2) indicated the presence of six methyl groups at δ_H 1.43 (s), 1.30 (s), 1.14 (s), 1.00 (s), 0.99 (s), and 0.86 (s) and one olefinic group at δ_H 5.72. The ^{13}C -NMR data of 3 (Table 2) indicated the presence of six methyl groups, two carboxylic carbons at δ_C 180.1 and 179.5, one carbonyl carbon at δ_C 216.3, and two olefinic carbons (one quaternary at δ_C 144.8 and one methine at δ_C 122.8, suggesting the presence of a double bond), 10 sp^3 methylenes, three sp^3 methines, and seven sp^3 quaternary carbon atoms. The NMR data of 3 were very similar to those of 3-oxo-olean-12-en-28,29-dioic acid [11], implying that 3 was also an oleanane triterpenoid.

Six fragments, C-1-C-2, C-5-C-6-C-7, C-9-C-11-C-12, C-15-C-16, C-18-C-19, and C-21-C-22, were deduced from the 1H - 1H COSY correlations in the 2D-NMR spectra of 3 (Figure 2). The structure of 3 was deduced as 3-oxo-olean-12-ene-28,30-dioic acid by the HMBC correlations from H_3 -23 and H_3 -24 to C-3, C-4, and C-5; from H_2 -1 and H_2 -2 to C-3; from H_3 -25 to C-1, C-5, C-9, and C-10; from H_3 -26 to C-7, C-9, and C-14; from H_3 -27 to C-8, C-13, and C-15; from H-18 to C-12, from H_2 -19 to C-17; from H_2 -16 and H_2 -22 to C-28; and from H_3 -29 to C-19, C-20, C-21 and C-30; as well as the key ROESY correlations of H -19 α / H_3 -27 and H -19 α / H_3 -29 (Figure 2).

The molecular formula of compound 4, $C_{31}H_{46}O_5$, with nine degrees of unsaturation, was determined by the ^{13}C -NMR data in methanol- d_4 (Table 2) and positive ion mode HRESIMS, which showed a pseudomolecular ion peak at m/z 521.3234 $[M + Na]^+$ (calcd. for $C_{31}H_{46}NaO_5$, 521.3237). The 1H -NMR data in methanol- d_4 (Table 2) showed signals for six methyl groups at δ_H 1.11 (s), 1.00 (s), 0.98 (s), 0.94 (s), 0.81 (s), and 0.78 (s); a methoxy group at δ_H 3.67 (s); and a disubstituted double bond at δ_H 6.33 (dd, $J = 11.2, 2.8$ Hz) and 5.72 (br d, $J = 11.2$ Hz). The NMR data (Table 2) were very similar to those of 30-*O*-methyl spergulagenate (27) [12]. However, compound 4 had one more degree of unsaturation than 30-*O*-methyl spergulagenate, which was supported by four olefinic carbons at δ_C 139.8, 130.8, 129.0, and 126.2 for two double bonds in the ^{13}C -NMR spectrum of 4 measured in methanol- d_4 . Finally, the structure of 4 was elucidated to be 3 β -hydroxyoleana-11,13(18)-diene-28,30-dioic acid 30-methyl ester by the key HMBC correlations from H-11 to C-10, from H-12 to C-8, and from H_3 -27 to C-13,

as well as the key ROESY correlations of H-3/H-5, H-5/H-9, H-9/H₃-27, H₃-29/H-19 α , H₃-29/H-16 α , and H₃-29/H₃-27 (Figure 2).

Table 2. ¹H and ¹³C-NMR data of **3** and **4** (δ in ppm, *J* in Hz).

No.	3 (Pyridine- <i>d</i> ₅)		4 (Methanol- <i>d</i> ₄)		4 (Pyridine- <i>d</i> ₅)	
	δ _H (500 MHz)	δ _C (126 MHz)	δ _H (600 MHz)	δ _C (151 MHz)	δ _H (500 MHz)	δ _C (126 MHz)
1	1.65 m 1.30 m	39.1	1.92 m 1.05 m	39.4	1.88 m 1.07 m	38.5
2	2.51 m 2.37 m	34.4	1.69 m 1.64 m	27.9	1.94 m 1.89 m	28.1
3		216.3	3.18 dd (11.7, 4.9)	79.8	3.49 dd (10.6, 5.0)	78.1
4		47.5		40.1		39.6
5	1.32 m	55.4	0.84 br d (12.1)	56.4	0.91 dd (12.2, 1.8)	55.3
6	1.35 m	19.8	1.63 m 1.46 m	19.6	1.61 m 1.44 m	18.8
7	1.46 m 1.31 m	32.7	1.35 m	33.7	1.31 m	32.9
8		39.7		42.2		41.2
9	1.70 m	47.2	1.99 br s	56.0	2.06 br s	54.9
10		36.9		38.0		37.1
11	1.88 m	23.8	5.72 br d (11.2)	129.0	5.78 br d (10.5)	127.8
12	5.72 br t (3.3)	122.8	6.33 dd (11.2, 2.8)	126.2	6.63 dd (10.5, 2.6)	125.7
13		144.8		139.8		138.3 ^a
14		42.2		43.6		42.7
15	2.18 m	28.5	1.72 m 1.08 m	26.2	1.97 m 1.08 m	25.6
16 α	2.19 m	24.0	1.71 m	33.8	1.78 m	33.1
16 β	2.08 m		1.95 m		2.25 m	
17		46.4		49.3 ^a		48.8
18	3.63 dd (13.7, 4.0)	43.5		130.8		131.2 ^a
19 α	1.92 dd (13.7, 13.7)		2.85 dd (14.5, 1.7)		3.18 d (15.2)	
19 β	2.50 m	43.1	2.17 d (14.5)	35.9	2.78 d (15.2)	35.6
20		44.1		44.8		43.9
21	2.41 m 1.47 m	31.2	1.83 m 1.57 m	33.0	2.28 m 1.78 m	32.5
22	2.41 m 2.08 m	34.8	2.29 m 1.41 m	35.4	2.67 ddd (13.8, 3.5, 3.5) 1.52 m	35.0
23	1.14 s	26.6	0.98 s	28.6	1.24 s	28.6
24	0.99 s	21.6	0.78 s	15.9	1.03 s	16.1
25	0.86 s	14.9	0.94 s	18.8	0.97 s	18.4
26	1.00 s	17.3	0.81 s	17.3	1.07 s	17.0
27	1.30 s	26.1	1.00 s	20.3	1.09 s	20.1
28		180.1		179.9		DAS ^b
29	1.43 s	29.1	1.11 s	20.4	1.28 s	20.2
30		179.5		180.4		178.5
30-OMe			3.67 s	52.6	3.60 s	51.8

^a Detected by HMBC. ^b Disappeared signal.

The HRESIMS of glinusopposide A (**5**) indicated a molecular formula of C₃₅H₅₈O₇, with the positive ion at *m/z* 613.4068 [M + Na]⁺ (calcd. for C₃₅H₅₈NaO₇, 613.4080). By comparing its NMR data (Table 3) with those of spergulagenin A 3-*O*- β -*D*-xylopyranoside (**31**) [13], compound **5** might be combined by a modified hopane and a β -xylopyranose [δ _H 4.87 d (*J* = 7.6 Hz)]. The configuration of xylopyranose in the plant was determined as the *D*-configuration by acidic hydrolysis of **31** followed by acetylation to yield 1,2,3,4-tetra-*O*-acetyl-*D*-xylopyranose. The genin was deduced as 16-deoxyspergulagenin A by ¹H-¹H COSY, HMBC, and ROESY experiments. The ROESY correlations (Figure 2) of H-3/H-5, H-5/H-9, H-9/H-12, H-12/H₃-28, and H₃-28/H₃-29 indicated that 3-OH, 12-OH, and Me-29 were β -, β -, and α -oriented, respectively. The xylose was located at 3-OH based on the HMBC correlations from H-3 to C-1' and from H-1' to C-3 (Figure 2). Finally, the structure of **5** was elucidated to be 16-deoxyspergulagenin A 3-*O*- β -*D*-xylopyranoside (glinusopposide A).

Both glinusopposides B (**6**) and C (**7**) have the same molecular formula, C₄₁H₆₈O₁₁, based on ¹³C-NMR data (Table 3) and HRESIMS. The NMR data of **6** and **7** (Table 3) indicated the presence of the same genin in the two saponins as in compound **5**, with differences in the sugars. There are two sugars, β -*D*-xylopyranose and α -*L*-rhamnopyranose, in the structures of **6** and **7**. Base

on the key HMBC correlations from H-1'' to C-2' and from H-1' to C-3 in **6**, along with the correlations from H-1'' to C-3' and from H-1' to C-3 in **7** (Supplementary Materials), the linkages between the two sugars were easily established to be Rha-(1→2)-Xyl-O-C-3 and Rha-(1→3)-Xyl-O-C-3 for saponins **6** and **7**, respectively. Therefore, the structures of **6** and **7** were determined to be 16-deoxyspergulenin A 3-O-[α -L-rhamnopyranosyl-(1→2)]- β -D-xylopyranoside (glinusopposide B) and 16-deoxyspergulenin A 3-O-[α -L-rhamnopyranosyl-(1→3)]- β -D-xylopyranoside (glinusopposide C), respectively.

Table 3. ^1H and ^{13}C -NMR data of **5–7** in Pyridine- d_5 (δ in ppm, J in Hz).

No.	5		6		7	
	δ_{H} (600 MHz)	δ_{C} (151 MHz)	δ_{H} (500 MHz)	δ_{C} (126 MHz)	δ_{H} (600 MHz)	δ_{C} (151 MHz)
1	1.70 m 0.97 m	39.3	1.63 m 0.90 m	39.1	1.67 m 0.94 m	39.3
2	2.21 m 1.91 m	27.4	2.13 m 1.88 m	27.0	2.14 m 1.87 m	27.3
3	3.38 dd (11.7, 4.4)	89.1	3.29 dd (11.8, 4.2)	88.6	3.31 dd (11.9, 4.4)	89.3
4		40.1		39.7		40.1
5	0.79 br d (11.9)	56.2	0.71 br d (9.3)	56.0	0.76 br d (12.0)	56.2
6	1.51 m 1.33 m	19.1	1.46 m 1.33 m	18.6	1.50 m 1.32 m	19.0
7	1.39 m 1.19 m	34.0	1.33 m 1.15 m	33.5	1.40 m 1.19 m	34.0
8		43.8		43.4		43.8
9	1.40 m	50.0	1.35 m	49.6	1.40 m	50.0
10		37.4		37.0		37.4
11	2.12 m 1.64 m	33.5	2.07 m 1.60 m	33.0	2.10 m 1.63 m	33.5
12	4.20 m	69.2	4.17 m	68.7	4.20 m	69.1
13	1.72 d (10.7)	56.9	1.68 d (11.1)	56.5	1.72 overlapped	57.0
14		42.1		41.6		42.1
15	1.51 m 1.20 m	34.8	1.48 m 1.17 m	34.4	1.52 m 1.21 m	34.8
16	1.44 m	20.2	1.42 m	19.8	1.46 m	20.2
17	1.82 dd (12.1, 2.9)	56.3	1.78 dd (11.9, 2.9)	55.9	1.82 dd (12.0, 2.8)	56.3
18		45.8		45.4		45.8
19	2.58 m 1.68 m	45.2	2.55 m 1.65 m	44.8	2.58 m 1.68 m	45.2
20	2.17 m 1.68 m	36.2	2.14 m 1.65 m	35.7	2.17 m 1.68 m	36.2
21		54.5		54.0		54.5
22		213.0		212.6		213.0
23	1.33 s	28.6	1.25 s	28.0	1.27 s	28.5
24	1.01 s	17.2	1.17 s	16.9	0.97 s	17.2
25	0.82 s	16.5	0.79 s	16.2	0.81 s	16.5
26	0.99 s	17.5	0.95 s	17.0	0.99 s	17.5
27	1.05 s	18.4	1.01 s	18.0	1.05 s	18.4
28	1.12 s	17.2	1.09 s	16.8	1.12 s	17.2
29	1.22 s	21.5	1.19 s	21.0	1.22 s	21.5
30	2.19 s	25.9	2.16 s	25.4	2.19 s	25.9
1'	4.87 d (7.6)	108.2	4.83 d (7.3)	106.2	4.77 d (7.5)	107.8
2'	4.05 dd (8.6, 7.6)	76.0	4.24 dd (8.2, 7.3)	78.0	4.04 dd (8.6, 7.5)	75.9
3'	4.20 m	79.1	4.18 m	79.7	4.32 dd (8.8, 8.8)	83.5
4'	4.26 m	71.7	4.15 m	71.6	4.17 m	70.2
5'	4.41 dd (11.3, 5.2)	67.6	4.33 m	67.0	4.36 m	67.4
	3.80 dd (11.3, 10.5)		3.71 dd (10.5, 9.9)		3.74 dd (11.2, 10.3)	
1''			6.54 d (0.9)	102.0	6.30 br s	103.2
2''			4.88 m	72.5	4.82 dd (3.4, 1.3)	73.1
3''			4.69 dd (9.5, 3.1)	72.6	4.62 dd (9.3, 3.4)	73.2
4''			4.35 m	74.2	4.37 dd (9.3, 9.3)	74.6
5''			4.77 m	69.8	5.01 m	70.4
6''			1.70 d (6.2)	18.8	1.71 d (6.2)	19.1
12-OH			5.23 d (6.2)			
2''-OH			6.69 br s			
4''-OH			6.72 br s			

Based on ^{13}C -NMR data (Table 4) and HRESIMS, the molecular formulae of glinusopposides D–G (8–11) were deduced to be $\text{C}_{43}\text{H}_{70}\text{O}_{13}$, $\text{C}_{45}\text{H}_{72}\text{O}_{13}$, $\text{C}_{47}\text{H}_{74}\text{O}_{14}$, and $\text{C}_{44}\text{H}_{70}\text{O}_{13}$, respectively. By comparing their NMR data (Table 4) with those of spergulagenin A 3-*O*- β -*D*-xylopyranoside (31) [13], saponins 8–11 were deduced to be disaccharide glycosides of spergulagenin A. The presence of *trans*-2-butenoyl (crotonyl) group in 9 was confirmed by the ^1H -NMR signals at δ_{H} 7.06 (m), 6.02 (dq, $J = 15.6, 1.6$ Hz), and 1.66 (3H, d, $J = 6.8$ Hz), along with COSY correlations of H-2'''/H-3''' and H-3'''/H-4''' (Supplementary Materials). The closely similar data and correlations can also be found in 10 and 11, herein the *trans*-2-butenoyl group was assigned in 10 and 11 as same way. The *trans*-2-butenoyl moiety of 9–11 was located at C-4' by the key HMBC correlation from H-4' to C-1'''. According to the correlations in the ^1H - ^1H COSY, HMBC, and ROESY spectra (Supplementary Materials), the structures of 8–11 were easily elucidated to be 3-*O*-[α -L-rhamnopyranosyl-(1 \rightarrow 3)-4-*O*-acetyl- β -*D*-xylopyranosyl] spergulagenin A (glinusopposide D), 3-*O*-[α -L-rhamnopyranosyl-(1 \rightarrow 3)-4-*O*-*trans*-2-butenoyl- β -*D*-xylopyranosyl] spergulagenin A (glinusopposide E), 3-*O*-[α -L-rhamnopyranosyl-(1 \rightarrow 3)-4-*O*-*trans*-2-butenoyl- β -*D*-xylopyranosyl] 12-*O*-acetylspergulagenin A (glinusopposide F), and 3-*O*-[β -*D*-xylopyranosyl-(1 \rightarrow 3)-4-*O*-*trans*-2-butenoyl- β -*D*-xylopyranosyl] spergulagenin A (glinusopposide G), respectively.

Table 4. ^1H and ^{13}C -NMR data of 8–11 in Pyridine- d_5 (δ in ppm, J in Hz).

No.	8		9		10		11	
	δ_{H} (500 MHz)	δ_{C} (126 MHz)	δ_{H} (500 MHz)	δ_{C} (126 MHz)	δ_{H} (800 MHz)	δ_{C} (201 MHz)	δ_{H} (800 MHz)	δ_{C} (201 MHz)
1	1.62 m 0.85 m	38.8	1.63 m 0.86 m	38.8	1.41 m 0.66 m	38.6	1.64 m 0.87 m	38.8
2	2.03 m 1.80 m	26.8	2.04 m 1.81 m	26.8	1.98 m 1.76 m	26.6	2.05 m 1.82 m	26.8
3	3.25 dd (11.8, 4.4)	88.8	3.26 dd (11.8, 4.4)	88.8	3.22 dd (11.9, 4.6)	88.8	3.29 dd (11.9, 4.0)	88.8
4		39.6		39.6		39.5		39.6
5	0.69 d (11.7)	55.7	0.69 br d (11.8)	55.7	0.64 m	55.5	0.70 br d (12.5)	55.7
6	1.43 m 1.27 m	18.6	1.44 m 1.27 m	18.6	1.41 m 1.23 m	18.4	1.41 m 1.31 m	18.6
7	1.40 m 1.21 m	33.6	1.41 m 1.22 m	33.6	1.35 m 1.17 m	33.3	1.42 m 1.23 m	33.6
8		45.7		45.7		45.8		45.7
9	1.33 m	49.1	1.34 m	49.1	1.28 m	48.5	1.35 m	49.1
10		36.9		36.9		36.8		36.9
11	2.07 m 1.62 m	33.0	2.09 m 1.63 m	33.0	1.98 m 1.37 m	28.1	2.09 m 1.63 m	33.0
12	4.19 m	68.6	4.21 m	68.6	5.47 m	72.2	4.20 m	68.6
13	1.79 d (10.7)	55.8	1.79 d (10.5)	55.8	1.90 d (11.5)	52.4	1.79 d (10.6)	55.8
14		41.8		41.8		41.6		41.7
15	1.87 m 1.69 m	45.7	1.88 m 1.70 m	45.7	1.83 m 1.64 m	45.2	1.88 m 1.70 m	45.6
16	4.12 m	65.5	4.11 m	65.5	4.06 m	65.0	4.12 m	65.5
17	2.28 d (11.3)	63.7	2.28 d (11.4)	63.7	2.23 d (11.5)	63.3	2.28 d (11.7)	63.7
18		47.1		47.1		46.4		47.1
19	2.61 m 1.87 m	45.8	2.63 m 1.90 m	45.8	1.83 m 1.68 m	44.8	2.62 m 1.89 m	45.7
20	2.05 m 1.74 m	37.6	2.06 m 1.74 m	37.6	2.04 m 1.66 m	37.5	2.06 m 1.73 m	37.6
21		53.6		53.6		53.4		53.6
22		214.9		215.0		214.6		214.9
23	1.22 s	28.0	1.22 s	28.0	1.21 s	27.9	1.25 s	28.0
24	0.89 s	16.6	0.90 s	16.6	0.88 s	16.6	0.94 s	16.7
25	0.76 s	16.0	0.76 s	16.0	0.72 s	15.9	0.77 s	16.0
26	0.98 s	17.0	0.99 s	17.0	0.93 s	16.8	0.99 s	17.0
27	1.11 s	19.2	1.11 s	19.2	1.08 s	18.9	1.12 s	19.1
28	1.21 s	17.8	1.21 s	17.8	1.03 s	17.7	1.21 s	17.8
29	1.66 s	21.0	1.66 s	21.0	1.61 s	20.9	1.66 s	21.0
30	2.34 s	26.3	2.34 s	26.3	2.37 s	26.3	2.35 s	26.3
1'	4.74 d (7.7)	107.2	4.76 d (7.5)	107.2	4.75 d (7.5)	107.2	4.83 d (7.3)	106.9
2'	4.00 m	75.9	4.00 dd (8.3, 7.5)	75.8	4.01 dd (8.4, 7.5)	75.8	4.08 m	75.0
3'	4.40 m	78.3	4.43 m	79.0	4.43 m	79.0	4.35 m	83.9
4'	5.28 ddd (9.7, 9.7, 5.5)	71.3	5.38 overlapped	71.0	5.39 m	70.9	5.44 m	70.7
5'	4.30 m 3.58 dd (11.3, 11.0)	63.1	4.35 m 3.63 dd (11.3 10.0)	63.2	4.38 m 3.65 m	63.2	4.35 m 3.68 m	63.3

Table 4. Cont.

No.	8		9		10		11	
	δ_H (500 MHz)	δ_C (126 MHz)	δ_H (500 MHz)	δ_C (126 MHz)	δ_H (800 MHz)	δ_C (201 MHz)	δ_H (800 MHz)	δ_C (201 MHz)
1''	6.26 d (1.2)	102.6	6.24 br s	102.8	6.25 br s	102.9	5.25 d (7.8)	106.9
2''	4.69 br s	72.4	4.74 dd (3.2, 1.4)	72.5	4.72 m	72.5	3.99 t (7.8)	75.8
3''	4.45 m	72.7	4.45 m	72.6	4.44 m	72.6	4.14 m	78.4
4''	4.30 t (9.3)	73.9	4.30 t (9.4)	73.9	4.29 dd (9.5, 9.5)	74.0	4.15 m	71.0
5''	4.43 m	70.0	4.40 m	70.0	4.40 m	70.1	4.31 m 3.70 m	67.6
6''	1.70 d (6.2)	18.8	1.68 d (6.3)	18.9	1.69 d (6.2)	18.9		
1'''		170.4		165.9		165.9		165.9
2'''	2.15 s	21.1	6.02 dq (15.6, 1.6)	122.7	6.04 br d (14.6)	122.8	5.99 br d (15.5)	123.1
3'''			7.06 m	146.0	7.07 m	145.9	7.09 m	145.4
4'''			1.66 d (6.8)	17.8	1.61 dd (7.0, 1.5)	17.8	1.61 br d (6.9)	17.8
1''''						170.4		
2''''					2.15 s	21.9		
12-OH	5.34 d (6.1)							
16-OH	5.49 d (5.0)							
2'-OH	7.68 d (6.1)							
2''-OH	6.80 br s							
4''-OH	6.80 br s							

Glinusopposide H (**12**) was assigned the molecular formula $C_{36}H_{58}O_8$, with eight degrees of unsaturation as determined by ^{13}C -NMR data (Table 5) and the positive ion at m/z 641.4021 [$M + Na$]⁺ (calcd. for $C_{36}H_{58}NaO_8$, 641.4024) in the HRESIMS. The 1H and ^{13}C -NMR data indicated the compound might be a hopane triterpenoid saponin with eight methyl groups [δ_H 1.67 (s), 1.20 (s), 1.44 (s), 1.44 (s), 0.99 (s), 0.94 (s), 0.88 (s), and 0.79 (s)], one tetrasubstituted double bond (δ_C 152.5 and 146.8), and one β -glucopyranose [δ_H 5.19 (d, $J = 7.6$ Hz); δ_C 100.1, 78.8, 78.4, 75.9, 72.4, and 63.4]. In addition to the signals for the sugar, signals (δ_C 84.2, 78.1, 76.0, and 74.5) for four oxygenated carbon atoms were observed. The sugar was attached to C-12 based on the HMBC correlations from H-12 to C-1' and from H-1' to C-12, and the 17(21)-double bond was confirmed by the correlations from H₃-28 to C-17 and from H₃-29 and H₃-30 to C-21 (Figure 2). The other three oxygenated carbon atoms were C-3, C-16, and C-22 based on the correlations from H₃-23 and H₃-24 to C-3, from H-16 to C-21, and from H₃-29 and H₃-30 to C-22. According to the deduced molecular formula and the degrees of unsaturation, a dihydrofuran ring containing the C-16-C-17-C-21-C-22-O fragment must be formed in the structure of **12**, which was further confirmed because of the shift in the ^{13}C -NMR signals for C-16 (δ_C 76.0) and C-22 (δ_C 84.2) to downfield compared with the analogues **1**, **2**, and 22,24,28-trihydroxy-hop-17(21)-ene [14]. The 3 β ,12 β ,16 β configurations were determined by the key ROESY correlations of H-3/H₃-23, H-3/H-5, H-5/H-9, H-9/H-12, H-12/H₃-27, H-12/H₃-28, H-16/H₃-27, and H-16/H₃-28 (Figure 2). Thus, the structure of **12** was elucidated to be 3 β ,12 β -dihydroxy-16 β ,22-epoxyhop-17(21)-ene 12-O- β -D-glucopyranoside (glinusopposide H).

Based on ^{13}C -NMR data (Tables 5 and 6) and HRESIMS, the molecular formulae of glinusopposides I–K (**13**–**15**) were deduced to be $C_{35}H_{56}O_7$, $C_{41}H_{66}O_{11}$, and $C_{41}H_{66}O_{11}$, respectively. Comparison of the NMR data of **13**–**15** (Tables 5 and 6) with those of **12** (Table 5) which are closely similar that were suggested these compounds with the same genin, 3 β ,12 β -dihydroxy-16 β ,22-epoxyhop-17(21)-ene. The position of connectivity of sugars to saponin were established according to the correlations in the 2D-NMR spectra (Supplementary Materials). Therefore, the structures of saponins **13**–**15** were determined to be 3 β ,12 β -dihydroxy-16 β ,22-epoxyhop-17(21)-ene 3-O- β -D-xylopyranoside (glinusopposide I), 3 β ,12 β -dihydroxy-16 β ,22-epoxyhop-17(21)-ene 3-O-[α -L-rhamnopyranosyl-(1 \rightarrow 2)]- β -D-xylopyranoside (glinusopposide J), and 3 β ,12 β -dihydroxy-16 β ,22-epoxyhop-17(21)-ene 3-O-[α -L-rhamnopyranosyl-(1 \rightarrow 3)]- β -D-xylopyranoside (glinusopposide K), respectively.

Table 5. ^1H and ^{13}C -NMR data of **12–14** in Pyridine- d_5 (δ in ppm, J in Hz).

No.	12		13		14	
	δ_{H} (500 MHz)	δ_{C} (126 MHz)	δ_{H} (600 MHz)	δ_{C} (151 MHz)	δ_{H} (600 MHz)	δ_{C} (151 MHz)
1	1.61 m 0.84 m	39.0	1.72 m 0.98 m	39.5	1.68 m 0.95 m	39.7
2	1.78 m	28.3	2.21 m 1.90 m	27.4	2.17 m 1.92 m	27.5
3	3.41 m	78.1	3.37 dd (11.8, 4.5)	89.0	3.31 dd (11.9, 4.2)	88.9
4		39.5		40.1		40.1
5	0.69 m	56.0	0.75 br d (10.8)	56.3	0.71 br d (11.5)	56.6
6	1.49 m 1.28 m	18.8	1.51 m 1.33 m	19.0	1.47 m 1.31 m	19.0
7	1.27 m	34.2	1.32 m	34.6	1.29 m	34.6
8		46.8		47.2		47.2
9	1.22 m	48.4	1.40 m	49.5	1.37 m	49.5
10		37.6		37.6		37.5
11	2.37 m 1.48 m	27.2	2.09 m 1.66 m	33.5	2.07 m 1.65 m	33.5
12	4.37 m	74.5	4.04 m	69.7	4.04 m	69.7
13	1.87 d (11.2)	54.0	1.92 d (11.1)	56.2	1.91 d (11.1)	56.2
14		41.5		41.9		41.9
15	1.92 m 1.29 m	43.0	1.99 dd (11.6, 6.2) 1.38 m	43.7	1.97 dd (11.7, 6.1) 1.36 m	43.7
16	4.84 m	76.0	4.93 m	76.6	4.92 m	76.6
17		152.5		153.0		153.0
18		46.0		46.4		46.4
19	2.88 m 2.54 m	53.7	3.15 m 2.70 m	54.6	3.15 m 2.70 ddd (13.6, 8.2, 2.6)	54.5
20	2.37 m 2.04 m	25.6	2.50 m 2.20 m	26.1	2.50 m 2.21 m	26.1
21		146.8		147.5		147.5
22		84.2		84.5		84.5
23	1.20 s	28.7	1.31 s	28.5	1.25 s	28.3
24	0.99 s	16.4	0.99 s	17.2	1.19 s	17.4
25	0.79 s	16.6	0.85 s	17.0	0.85 s	17.1
26	0.88 s	16.5	1.02 s	16.9	1.01 s	16.9
27	0.94 s	15.9	1.07 s	16.2	1.06 s	16.2
28	1.67 s	22.2	1.59 s	23.0	1.59 s	23.0
29	1.44 s	29.2	1.49 s	29.2	1.49 s	29.2
30	1.44 s	28.6	1.47 s	29.5	1.47 s	29.5
1'	5.19 d (7.5)	100.1	4.86 d (7.5)	108.2	4.85 d (7.4)	106.6
2'	4.07 m	75.9	4.05 m	76.0	4.27 dd (8.3, 7.4)	78.4
3'	4.37 m	78.8	4.20 dd (8.7, 8.7)	79.1	4.20 dd (8.7, 8.3)	80.1
4'	4.26 dd (9.5, 9.5)	72.4	4.26 m	71.7	4.17 m	72.0
5'	4.05 m	78.4	4.39 dd (11.3, 5.2) 3.79 dd (11.3, 10.7)	67.6	4.34 dd (11.4, 4.8) 3.73 dd (11.4, 9.9)	67.4
6'	4.57 dd (11.7, 2.2) 4.36 m	63.4				
1''					6.58 br s	102.4
2''					4.90 dd (3.4, 1.4)	72.9
3''					4.71 dd (9.4, 3.4)	73.0
4''					4.38 dd (9.3, 9.3)	74.6
5''					4.80 m	70.2
6''					1.73 d (6.2)	19.2
12-OH					5.46 br s	

The HRESIMS of glinusoposide L (**16**) exhibited an ion peak at m/z 731.4353 $[\text{M} + \text{Na}]^+$ (calcd. for $\text{C}_{39}\text{H}_{64}\text{NaO}_{11}$, 731.4346), implying a molecular formula of $\text{C}_{39}\text{H}_{64}\text{O}_{11}$. The NMR data of **16** (Table 6) were highly similar to those of spergulin B (**35**) [13], indicating that the compound might also be a bisnor hopane saponin with the same genin, spergulatriol, and the same sugars, xylose and rhamnose. The difference between the two saponins was the linkage mode of the two sugars. The rhamnose was linked to 3-OH of the inner sugar, xylose, based on the HMBC correlations from H-1'' to C-3' and from

H-3' to C-1'' (Supplementary Materials). Finally, the structure of **16** was elucidated to be spergulatriol 3-O-[α -L-rhamnopyranosyl-(1 \rightarrow 3)]- β -D-xylopyranoside (glinusopposide L).

According to ^{13}C -NMR data (Table 6) and the positive ion HRESIMS at m/z 731.4347 [$\text{M} + \text{Na}$] $^+$ (calcd. for $\text{C}_{39}\text{H}_{64}\text{NaO}_{11}$, 731.4346), glinusopposide M (**17**) had the same molecular formula, $\text{C}_{39}\text{H}_{64}\text{O}_{11}$, as saponin **16**. The 1D and 2D-NMR spectra (Supplementary Materials) indicated that **17** had a tetrasubstituted double bond rather than the terminal double bond of **16**. The 17(21) double bond was identified based on the HMBC correlations from H₃-28 to C-17 and from H₃-22 to C-17 and C-21. Therefore, the structure of **17** was determined to be 29,30-bisnor-3 β ,12 β ,16 β -trihydroxyhop-17(21)-ene 3-O-[α -L-rhamnopyranosyl-(1 \rightarrow 3)]- β -D-xylopyranoside (glinusopposide M).

Table 6. ^1H and ^{13}C -NMR data of **15–17** in Pyridine- d_5 (δ in ppm, J in Hz).

No.	15		16		17	
	δ_{H} (600 MHz)	δ_{C} (151 MHz)	δ_{H} (500 MHz)	δ_{C} (126 MHz)	δ_{H} (800 MHz)	δ_{C} (201 MHz)
1	1.69 m 0.95 m	39.5	1.64 m 0.90 m	38.8	1.63 m 0.91 m	39.0
2	2.14 m 1.87 m	27.3	2.11 m 1.83 m	26.8	2.10 m 1.83 m	26.9
3	3.30 dd (11.9, 4.3)	89.2	3.27 dd (11.8, 4.4)	88.8	3.26 dd (12.0, 4.3)	88.8
4		40.1		39.6		39.6
5	0.73 br d (11.3)	56.3	0.72 br d (11.9)	55.7	0.73 br d (11.7)	55.9
6	1.48 m 1.31 m	19.0	1.47 m 1.30 m	18.6	1.44 m 1.30 m	18.6
7	1.31 m	34.6	1.45 m 1.27 m	33.5	1.40 m 1.31 m	33.6
8		47.2		45.4		44.8
9	1.39 m	49.5	1.38 m	49.2	1.47 m	49.6
10		37.5		36.9		37.0
11	2.09 m 1.65 m	33.5	2.07 m 1.61 m	33.1	2.08 m 1.62 m	33.4
12	4.04 m	69.7	4.19 m	69.3	4.08 m	69.6
13	1.92 d (11.1)	56.2	1.77 d (10.9)	53.9	1.91 m	55.1
14		47.2		41.8		41.7
15	2.00 m 1.38 m	43.7	1.87 dd (12.5, 4.2) 1.73 m	45.1	1.92 m 1.87 m	44.1
16	4.93 m	76.6	4.32 m	67.2	4.99 overlapped	68.1
17		153.0	2.14 d (10.8)	62.2		143.9
18		46.4		45.4		52.6
19	3.15 m 2.70 m	54.6	2.53 m 1.78 m	43.2	2.58 m 2.20 m	46.5
20	2.50 m 2.21 m	26.1	2.42 m	29.9	2.54 m 2.18 m	38.1
21		147.5		152.2		128.5
22		84.5	6.06 t (2.0) 5.14 t (2.0)	106.1	2.33 s	16.0
23	1.25 s	28.4	1.23 s	28.0	1.21 s	28.0
24	0.95 s	17.2	0.93 s	16.7	0.92 s	16.7
25	0.83 s	17.0	0.78 s	16.0	0.79 s	16.4
26	1.02 s	16.9	1.01 s	17.0	0.98 s	16.5
27	1.07 s	16.2	1.16 s	19.1	1.25 s	17.5
28	1.59 s	23.0	1.06 s	16.0	1.39 s	20.6
29	1.49 s	29.2				
30	1.47 s	29.5				
1'	4.76 d (7.5)	107.8	4.74 d (7.4)	107.4	4.73 d (7.5)	107.4
2'	4.03 m	75.9	4.01 m	75.4	4.00 m	75.4
3'	4.32 dd (8.9, 8.9)	83.5	4.30 t (8.9)	83.0	4.29 t (8.8)	83.0
4'	4.16 m	70.2	4.14 m	69.7	4.13 m	69.7
5'	4.35 m 3.73 dd (11.2, 10.4)	67.4	4.32 m 3.72 dd (11.3, 10.2)	67.0	4.33 m 3.71 dd (11.2, 10.3)	66.9

Table 6. Cont.

No.	15		16		17	
	δ_H (600 MHz)	δ_C (151 MHz)	δ_H (500 MHz)	δ_C (126 MHz)	δ_H (800 MHz)	δ_C (201 MHz)
1''	6.30 br s	103.3	6.26 d (1.2)	102.9	6.26 br s	102.8
2''	4.82 dd (3.3, 1.5)	73.1	4.78 br s	72.6	4.78 br s	72.6
3''	4.62 dd (9.4, 3.3)	73.2	4.60 br d (9.1)	72.8	4.59 br d (8.7)	72.8
4''	4.37 dd (9.4, 9.4)	74.6	4.34 m	74.2	4.33 m	74.2
5''	5.00 m	70.4	4.98 overlapped	70.0	4.97 overlapped	70.0
6''	1.71 d (6.2)	19.2	1.68 d (6.2)	18.7	1.68 d (6.1)	18.7
12-OH			5.27 d (6.5)		5.20 d (6.2)	
16-OH			5.72 d (5.9)		6.03 d (5.5)	
2'-OH			7.29 d (6.0)		7.26 d (6.0)	
4'-OH			6.79 d (5.9)		6.76 d (5.6)	
2''-OH			6.74 br s		6.71 br s	
3''-OH			6.47 br s		6.43 br s	
4''-OH			6.74 br s		6.71 br s	

According to ^{13}C -NMR data (Table 7) and HRESIMS, the molecular formulae of glinusoposides N (18) and O (19) were deduced to be $\text{C}_{33}\text{H}_{52}\text{O}_6$ and $\text{C}_{39}\text{H}_{62}\text{O}_{10}$, respectively. Comparison of their NMR data (Table 7) with those of 17 indicated that saponins 18 and 19 were 29,30-bisnor hopane saponins with two double bonds and two hydroxy substitutions in the structure of the genin. 3β -OH and 12β -OH were determined based on the key HMBC correlations from H_3 -23 and H_3 -24 to C-3 and from H-9 to C-12, as well as the key ROESY correlations of H-3/H-5, H-5/H-9, H-9/H-12, H-12/ H_3 -27, and H-12/ H_3 -28 (Supplementary Materials). The 15,17(21) double bonds were identified by the HMBC correlations from H_3 -22 to C-17 and C-21, from H_3 -27 to C-15, from H_3 -28 to C-17, and from H-16 to C-14 and C-18. Finally, based on other correlations in the 2D-NMR spectra (Supplementary Materials), 18 and 19 were elucidated to be 29,30-bisnor- $3\beta,12\beta$ -dihydroxyhopa-15,17(21)-diene 3-O- β -D-xylopyranoside (glinusoposide N) and 29,30-bisnor- $3\beta,12\beta$ -dihydroxyhopa-15,17(21)-diene 3-O- $[\alpha$ -L-rhamnopyranosyl-(1 \rightarrow 3)]- β -D-xylopyranoside (glinusoposide O), respectively.

The molecular formula of glinusoposide P (20) was determined to be $\text{C}_{44}\text{H}_{66}\text{O}_{15}$ based on ^{13}C -NMR data (Table 7) and the positive ion at m/z 857.4300 $[\text{M} + \text{Na}]^+$ (calcd. for $\text{C}_{44}\text{H}_{66}\text{NaO}_{15}$, 857.4299) in the HRESIMS. The NMR data (Table 7) indicated a moiety of 3β -hydroxyoleana-11,13(18)-diene-28,30-dioic acid 30-methyl ester (4), an α -rhamnopyranosyl group [δ_H 6.33 (br s), 5.08 (m), 4.76 (dd, $J = 3.3, 1.4$ Hz), 4.57 (dd, $J = 9.3, 3.3$ Hz), 4.35 (dd, $J = 9.3, 9.3$ Hz), and 1.71 (d, $J = 6.1$ Hz); δ_C 103.4, 74.6, 73.2, 73.0, 70.3, and 19.1], and a 6-O-methyl- β -glucuronopyranosyl group [δ_H 4.92 (d, $J = 7.9$ Hz), 4.58 (d, $J = 9.3$ Hz), 4.45 (dd, $J = 9.3, 8.7$ Hz), 4.41 (dd, $J = 9.3, 9.3$ Hz), 4.07 (dd, $J = 8.7, 7.9$ Hz), and 3.79 (s); δ_C 171.3, 107.6, 82.3, 77.6, 76.2, 71.9, and 52.7]. The linkage of the sugar chain was determined to be Rha-(1 \rightarrow 3)-[6-O-methyl-GlcA]-O-C-3 based on the key HMBC correlations from H-1'' to C-3', from H-3' to C-1'', from H-1' to C-3, and from H-3 to C-1' (Supplementary Materials). Thus, the structure of 20 was elucidated to be 3-O- $[\alpha$ -L-rhamnopyranosyl-(1 \rightarrow 3)-6-O-methyl- β -D-glucuronopyranosyl]- 3β -hydroxyoleana-11,13(18)-diene-28,30-dioic acid 30-methyl ester (glinusoposide P).

Table 7. ^1H and ^{13}C -NMR data of 18–20 in Pyridine- d_5 (δ in ppm, J in Hz).

No.	18		19		20	
	δ_H (600 MHz)	δ_C (151 MHz)	δ_H (500 MHz)	δ_C (126 MHz)	δ_H (J in Hz) (600 MHz)	δ_C (151 MHz)
1	1.69 m	39.2	1.61 m	38.8	1.70 m	38.5
	0.98 m		0.90 m		0.89 m	
2	2.21 m	27.4	2.10 m	26.9	2.14 m	27.0
	1.91 m		1.82 m		1.87 m	
3	3.39 dd (11.9, 4.3)	89.1	3.27 dd (11.9, 4.4)	88.8	3.32 dd (11.9, 4.5)	89.8
4		40.2		39.7		40.1
5	0.84 m	56.5	0.77 overlapped	56.0	0.79 br d (12.1)	55.6

Table 7. Cont.

No.	18		19		20	
	δ_H (600 MHz)	δ_C (151 MHz)	δ_H (500 MHz)	δ_C (126 MHz)	δ_H (J in Hz) (600 MHz)	δ_C (151 MHz)
6	1.57 m	19.1	1.54 m	18.6	1.52 m	18.8
	1.42 m		1.37 m		1.33 m	
7	1.52 m	33.9	1.48 m	33.5	1.28 m	33.2
8		41.8		41.3		41.6
9	1.50 m	50.2	1.45 m	49.7	1.98 br s	55.2
10		37.7		37.3		37.1
11	2.18 m	34.3	2.14 m	33.9	5.69 br d (10.1)	128.2
	1.66 m		1.61 m			
12	4.33 m	69.4	4.28 m	69.0	6.60 dd (10.1, 2.9)	126.2
13	2.17 d (11.1)	53.3	2.13 d (11.1)	52.8		138.7
14		47.5		47.0		43.1
15	5.76 d (10.3)	135.5	5.72 d (10.3)	135.1	1.96 m	26.0
					1.09 m	
16	6.42 d (10.3)	120.4	6.39 d (10.3)	120.0	2.26 m	33.5
					1.78 m	
17		141.9		141.5		49.2
18		48.6		48.2		131.4
19	2.59 m	45.3	2.55 m	44.9	3.17 d (14.5)	36.0
	2.24 m		2.21 m		2.77 d (14.5)	
20	2.60 m	36.8	2.55 m	36.3		44.3
	2.14 m		2.09 m			
21		131.8		131.4	2.31 m	32.9
					1.79 m	
22	1.73 s	14.4	1.70 s	14.0	2.66 m	35.3
					1.52 m	
23	1.35 s	28.6	1.25 s	28.0	1.25 s	28.2
24	1.02 s	17.2	0.94 s	16.7	0.89 s	16.8
25	0.81 s	16.3	0.76 s	15.9	0.84 s	18.7
26	1.03 s	19.7	0.99 s	19.3	1.02 s	17.4
27	1.34 s	19.5	1.30 s	19.0	1.11 s	20.5
28	1.32 s	20.4	1.29 s	20.0		179.1
29					1.27 s	20.7
30						178.9
30-Me					3.60 s	52.2
1'	4.88 d (7.7)	108.2	4.74 d (7.5)	107.4	4.92 d (7.9)	107.6
2'	4.05 dd (8.4, 7.7)	76.0	4.00 dd (8.4, 7.5)	75.4	4.07 dd (8.7, 7.9)	76.2
3'	4.20 dd (8.8, 8.4)	79.1	4.28 m	83.0	4.45 dd (9.3, 8.7)	82.3
4'	4.26 m	71.7	4.12 m	69.7	4.41 dd (9.3, 9.3)	71.9
			4.32 m			
5'	4.40 dd (11.0, 5.1)	67.6	3.70 dd (11.0, 10.5)	67.0	4.58 d (9.3)	77.6
	3.80 dd (11.0, 10.4)					
6'						171.3
6'-OMe					3.79 s	52.7
1''			6.27 br s	102.8	6.33 br s	103.4
2''			4.79 br s	72.6	4.76 dd (3.3, 1.4)	73.0
3''			4.59 dd (9.3, 3.0)	72.8	4.57 dd (9.3, 3.3)	73.2
4''			4.34 dd (9.3, 9.3)	74.2	4.35 dd (9.3, 9.3)	74.6
5''			4.97 m	69.9	5.08 m	70.3
6''			1.67 d (6.1)	18.7	1.71 d (6.1)	19.1

Based on ^{13}C -NMR data (Tables 8 and 9) and HRESIMS, the molecular formulae of glinusoposides Q–U (21–25) were deduced to be $\text{C}_{39}\text{H}_{61}\text{NO}_{10}$, $\text{C}_{44}\text{H}_{68}\text{O}_{15}$, $\text{C}_{45}\text{H}_{70}\text{O}_{15}$, $\text{C}_{36}\text{H}_{56}\text{O}_9$, and $\text{C}_{42}\text{H}_{66}\text{O}_{13}$, respectively. By comparing their NMR data with those of 30-O-methyl spergulagenate (27) [12], these saponins were determined to have the same genin, 30-O-methyl spergulagenate. The NMR signals of 21 at δ_H 8.94 (d, $J = 9.0$ Hz) and 2.15 (s), along with δ_C 170.3 and 23.8 manifested the presence of an acetylamino unit which was further confirmed by the HMBC correlations from δ_H 2.15 (H-2'') to δ_C 170.3 (C-1'') and from δ_H 8.94 (NH) to δ_C 170.3 (C-1''). The position of the acetylamino moiety of 21 was determined by the HMBC correlation from H-2' to C-1''. The location of the sugar in 21 was also confirmed by the HMBC correlations from H-3 to C-1' and H-1' to C-3. Two anomeric carbons at δ_C 107.1 and 102.9 of 22 suggested that the presence of two sugars,

of which the positions were assigned by the key HMBC from H-3' to C-1'', from H-1'' to C-3', from H-1' to C-3, and from H-3 to C-1'. The NMR data of **23** were almost identical to those of **22** except for the replacement of the methoxy group in **22** by ethoxy group (δ_C 61.4 and 14.3). Comparison of NMR data of 30-O-methyl spergulagenate (**27**), signals for an additional sugar in compound **24** and for two additional sugars in compound **25** were observed. According to these correlations in the 2D-NMR spectra (Supplementary Materials), saponins **21–25** were determined as 3-O-(2-acetylamino-2-deoxy- β -D-glucopyranosyl)-30-O-methyl spergulagenate (glinusopposide Q), 3-O-[α -L-rhamnopyranosyl-(1 \rightarrow 3)-6-O-methyl- β -D-glucuronopyranosyl]-30-O-methyl spergulagenate (glinusopposide R), 3-O-[α -L-rhamnopyranosyl-(1 \rightarrow 3)-6-O-ethyl- β -D-glucuronopyranosyl]-30-O-methyl spergulagenate (glinusopposide S), 30-O-methyl spergulagenate 3-O- β -D-xylopyranoside (glinusopposide T), and 30-O-methyl spergulagenate 3-O-[α -L-rhamnopyranosyl-(1 \rightarrow 3)]- β -D-xylopyranoside (glinusopposide U), respectively.

Table 8. ^1H and ^{13}C -NMR data of **21–23** in Pyridine- d_5 (δ in ppm, J in Hz).

No.	21		22		23	
	δ_H (500 MHz)	δ_C (126 MHz)	δ_H (500 MHz)	δ_C (126 MHz)	δ_H (500 MHz)	δ_C (126 MHz)
1	1.35 m 0.82 m	38.6	1.36 m 0.82 m	38.5	1.37 m 0.83 m	38.5
2	2.19 m 1.76 m	26.4	2.04 m 1.77 m	26.6	2.07 m 1.78 m	26.6
3	3.25 dd (11.9, 4.4)	89.2	3.28 overlapped	89.4	3.27 overlapped	89.3
4		39.3		39.5		39.5
5	0.75 overlapped	55.8	0.75 overlapped	55.7	0.74 overlapped	55.7
6	1.49 m 1.28 m	18.6	1.46 m 1.25 m	18.4	1.46 m 1.26 m	18.4
7	1.46 m 1.27 m	33.3	1.44 m 1.26 m	33.2	1.45 m 1.26 m	33.2
8		39.7		42.1		42.1
9	1.60 m	48.1	1.61 m	48.0	1.62 dd (8.6, 8.6)	48.0
10		37.0		36.9		36.9
11	1.85 m	23.8	1.85 m	23.7	1.85 m	23.7
12	5.58 br s	122.5	5.59 br s	123.1	5.59 dd (3.4, 3.4)	123.1
13		145.5		144.5		144.5
14		42.2		39.7		39.7
15	2.21 m	28.6	2.12 m 1.18 m	28.4	2.13 m 1.27 m	28.4
16	2.08 m	24.2	2.12 m 2.02 m	23.9	2.13 m 2.03 m	23.9
17		46.4		46.2		46.2
18	3.36 dd (13.5, 3.6)	43.6	3.29 overlapped	43.4	3.29 overlapped	43.4
19	2.26 m 1.82 m	43.2	2.25 br d (13.2) 1.81 m	42.7	2.25 br d (12.0) 1.82 m	42.7
20		44.3		44.2		44.2
21	2.16 m 1.45 m	31.2	2.19 m 1.46 m	30.9	2.19 br d (13.5) 1.47 m	30.9
22	2.06 m 1.96 m	34.9	2.08 m 1.97 m	34.6	2.09 m 1.98, m	34.6
23	1.19 s	28.2	1.24 s	28.1	1.23 s	28.1
24	0.98 s	17.0	0.90 s	16.9	0.90 s	16.9
25	0.75 s	15.4	0.75 s	15.4	0.76 s	15.4
26	0.89 br s	17.6	0.95 s	17.3	0.95 s	17.3
27	1.31 s	26.2	1.31 s	26.2	1.31 s	26.2
28		DAP ^a		179.9		179.9
29	1.22 s	28.7	1.23 s	28.5	1.23 s	28.5
30		177.4		177.2		177.2
30-OMe	3.63 s	51.7	3.65 s	51.8	3.65 s	51.7
1'	5.05 d (8.2)	105.0	4.88 d (7.8)	107.1	4.88 d (7.9)	107.2
2'	4.58 m	58.1	4.34 m	74.1	4.05 dd (8.4, 7.9)	75.8
3'	4.41 dd (9.3, 8.7)	76.3	4.42 dd (9.0, 9.0)	81.9	4.44 dd (8.9, 8.4)	81.9
4'	4.18 dd (9.3, 9.3)	72.7	4.37 m	71.4	4.41 dd (9.4, 8.9)	71.4

Table 8. Cont.

No.	21		22		23	
	δ_H (500 MHz)	δ_C (126 MHz)	δ_H (500 MHz)	δ_C (126 MHz)	δ_H (500 MHz)	δ_C (126 MHz)
5'	3.97 m	78.4	4.56 d (9.4)	77.2	4.55 d (9.4)	77.2
6'	4.57 m 4.37 m	63.0		170.8		170.3
6'-OMe, OEt			3.77 s	52.2	4.29 m	61.4
1''		170.3	6.30 br s	102.9	1.19 t (7.1)	14.3
2''	2.15 s	23.8	4.75 m	72.5	6.33 d (1.2)	102.8
3''			4.55 m	72.7	4.77 dd (3.4, 1.2)	72.6
4''			4.34 m	74.1	4.56 dd (9.2, 3.4)	72.7
5''			5.05 m	69.9	4.36 dd (9.2, 9.2)	74.1
6''			1.69 d (6.1)	18.6	5.08 m	69.8
NH	8.94 d (9.0)				1.69 d (6.2)	18.7

^a Disappeared.Table 9. ¹H- and ¹³C-NMR data of 24–26 in Pyridine-*d*₅ (δ in ppm, *J* in Hz).

No.	24		25		26	
	δ_H (500 MHz)	δ_C (126 MHz)	δ_H (500 MHz)	δ_C (126 MHz)	δ_H (500 MHz)	δ_C (126 MHz)
1	1.51 m 0.97 m	38.8	1.47 m 0.93 m	38.7	1.39 m 0.85 m	38.6
2	2.16 m 1.87 m	26.8	2.09 m 1.81 m	26.7	2.13 m 1.83 m	26.6
3	3.35 dd (11.7, 4.4)	88.7	3.28 overlapped	88.8	3.36 dd (11.6, 4.3)	89.2
4		39.6		39.5		39.6
5	0.82 overlapped	55.9	0.79 overlapped	55.8	0.79 overlapped	55.8
6	1.49 m 1.28 m	18.5	1.47 m 1.27 m	18.5	1.47 m 1.26 m	18.5
7	1.47 m 1.28 m	33.2	1.46 m 1.27 m	33.2	1.45 m 1.27 m	33.2
8		39.7		42.0		39.7
9	1.67 dd (9.0, 8.7)	48.1	1.65 m	48.0	1.63 dd (9.0, 8.6)	48.0
10		37.1		37.0		37.0
11	1.89 m	23.8	1.88 m	23.7	1.87 m	23.7
12	5.60 br t (3.1)	123.2	5.60 dd (3.4, 3.4)	123.1	5.60 br t (3.3)	123.1
13		144.5		144.4		144.5
14		42.1		39.7		42.1
15	2.13 m 1.19 m	28.4	2.13 m 1.27 m	28.4	2.13 m 1.20 m	28.4
16	2.13 m 2.03 m	23.9	2.12 m 2.02 m	23.8	2.12 m 2.03 m	23.9
17		46.2		46.2		46.2
18	3.30 dd (13.6, 3.6)	43.4	3.29 overlapped	43.4	3.29 dd (13.6, 3.9)	43.4
19	2.26 m 1.82 dd (13.6, 13.6)	42.7	2.26 br d (13.5) 1.82 dd (13.5, 13.5)	42.7	2.26 m 1.82 m	42.7
20		44.2		44.2		44.2
21	2.19 m 1.46 m	30.9	2.19 br d (13.1) 1.46 m	30.8	2.20 m 1.46 m	30.9
22	2.10 m 1.98 m	34.6	2.09 m 1.98 m	34.5	2.09 m 1.98 m	34.6
23	1.30 s	28.2	1.24 s	28.1	1.30 s	28.2
24	0.97 s	17.0	0.92 s	16.9	0.95 s	17.0
25	0.82 s	15.5	0.80 s	15.5	0.78 s	15.5
26	0.97 s	17.4	0.96 s	17.3	0.95 s	17.4
27	1.30 s	26.2	1.30 s	26.1	1.30 s	26.2
28		179.9		179.9		179.9
29	1.23 s	28.5	1.23 s	28.5	1.23 s	28.5
30		177.2		177.2		177.2
30-OMe	3.65 s	51.8	3.64 s	51.7	3.65 s	51.8

Table 9. Cont.

No.	24		25		26	
	δ_H (500 MHz)	δ_C (126 MHz)	δ_H (500 MHz)	δ_C (126 MHz)	δ_H (500 MHz)	δ_C (126 MHz)
1'	4.83 d (7.6)	107.8	4.73 d (7.5)	107.4	5.00 d (7.8)	107.3
2'	4.01 dd (8.7, 7.6)	75.6	4.00 dd (8.8, 7.5)	75.4	4.09 dd (9.0, 7.8)	75.4
3'	4.17 dd (8.7, 8.7)	78.7	4.29 dd (8.8, 8.8)	82.9	4.28 dd (9.0, 9.0)	77.9
4'	4.23 m	71.3	4.13 m	69.7	4.48 dd (9.0, 9.7)	73.3
5'	4.38 dd (11.2, 5.1) 3.78 dd (11.2, 10.2)	67.2	4.34 m 3.73 dd (10.6, 10.2)	66.9	4.61 d (9.7)	77.3
6'						170.9
6'-OMe					3.73 s	52.1
1''			6.27 d (1.2)	102.7		
2''			4.79 dd (3.3, 1.2)	72.6		
3''			4.60 dd (9.3, 3.3)	72.7		
4''			4.34 dd (9.3, 9.3)	74.1		
5''			4.98 m	69.9		
6''			1.67 d (6.2)	18.7		

The NMR data of compound **26** in methanol- d_4 (Supplementary Materials) were the same as those of coryternic acid 3-*O*- β -*D*-glucuronopyranoside-6'-*O*-methyl ester [3 β -*O*-(6-*O*-methyl- β -*D*-glucuronopyranosyl)-olean-12-ene-28,29-dioic acid 29-methyl ester] [15]. Based on the 1D and 2D-NMR spectra of **26** both in methanol- d_4 and pyridine- d_5 (Table 9, Figure 2, and Supplementary Materials), especially on the ROSEY correlations of H₃-29/H-19 α and H-19 α /H₃-27, the structure of **26** was determined to be 3 β -*O*-(6-*O*-methyl- β -*D*-glucuronopyranosyl)-olean-12-ene-28,30-dioic acid 30-methyl ester. Therefore, the structure of coryternic acid 3-*O*- β -*D*-glucuronopyranoside-6'-*O*-methyl ester reported in the literature is suggested to be revised to 3 β -*O*-(6-*O*-methyl- β -*D*-glucuronopyranosyl)-olean-12-ene-28,30-dioic acid 30-methyl ester.

Other known compounds, 30-*O*-methyl spergulagenate (**27**) [12], 28- β -*D*-glucopyranosyl-30-methyl 3 β -hydroxyolean-12-en-28,30-dioate (**28**) [16], oleanolic acid 3-*O*-6'-*O*-methyl- β -*D*-glucuronopyranoside (**29**) [17], oppositifolone (**30**) [18], spergulagenin A 3-*O*- β -*D*-xylopyranoside (**31**) [13], spergulin A (**32**) [13], spergulacin A (**33**) [13], spergulacin (**34**) [13], spergulin B (**35**) [13], grasshopper ketone (**36**) [19], and β -carboline (**37**) [20], were determined by comparing their NMR data (for all compounds) and optical rotation values (for all compounds except **37**) with those reported in the literature.

2.2. Biological Evaluation

We proposed antifungal activities of *G. oppositifolius* according to traditional healthcare use. The 70% ethanol extract of the whole plants of *G. oppositifolius* showed inhibitory activity against *M. gypseum* with an inhibition of $23.0 \pm 1.9\%$ at a concentration of 128 $\mu\text{g/mL}$. All the isolated compounds (**1**–**37**) were measured for antifungal activities against *M. gypseum* and *T. rubrum*, and the results are presented in Table 10. Glinusopposide B (**6**), glinusopposide Q (**21**), glinusopposide T (**24**), and glinusopposide U (**25**) showed the most notable inhibitory activities against *M. gypseum* (MIC₅₀ 7.1, 6.7, 6.8, and 11.1 μM , respectively) and *T. rubrum* (MIC₅₀ 14.3, 13.4, 11.9, and 13.0 μM , respectively) compared with the positive control terbinafine hydrochloride (MIC₅₀ 0.008 μM against *M. gypseum* and 1.647 μM against *T. rubrum*). Glinusopposide K (**15**), glinusopposide N (**18**), glinusopposide O (**19**), glinusopposide R (**22**), glinusopposide S (**23**), glinusopposide U (**25**), and 3 β -*O*-(6-*O*-methyl- β -*D*-glucuronopyranosyl)-olean-12-ene-28,30-dioic acid 30-methyl ester (**26**) showed moderate inhibitory activities against *M. gypseum*, with MIC₅₀ values ranging from 22.0 to 46.8 μM . Additionally, 3 β ,12 β ,16 β ,21 β ,22-pentahydroxyhopane (**1**), 3-oxo-olean-12-ene-28,30-dioic acid (**3**), glinusopposide H (**12**), and glinusopposide L (**16**) showed weak activities against *M. gypseum*, with MIC₅₀ values ranging from 105.0 to 260.1 μM . Other compounds did not display activity against *M. gypseum* or *T. rubrum* (MIC₅₀ > 300 μM).

The active compounds of *G. oppositifolius* against *M. gypseum* and *T. rubrum* have two types of carbon skeletons, hopane and oleanane. For those oleanane-type compounds, glycosylation (**21**–**26**) or

oxidation (**3**) of 3-OH was helpful in increasing the activity based on a comparison of the MIC₅₀ values of **3** and **21–26** with those of **27** and **28**. Replacement of the 30-methyl group (**29**) with a carboxymethyl group (**26**) enhanced the activity. The presence of 11,13(18) double bonds (**20**) decreased the activity. The structure-activity relationships (SARs) of the hopane-type compounds against the two fungi were not clear.

Table 10. Antifungal Effects of Compounds from *G. oppositifolius* against *Microsporum gypseum* and *Trichophyton rubrum*^a.

Compound	MIC ₅₀ (μM) ± SD	
	<i>M. gypseum</i>	<i>T. rubrum</i>
1	105.0 ± 0.6	>300
3	128.1 ± 1.4	>300
6	7.1 ± 1.2	14.3 ± 2.1
12	260.1 ± 2.3	>300
15	46.8 ± 0.1	>300
16	120.7 ± 1.4	>300
18	29.3 ± 3.4	>300
19	34.9 ± 1.2	>300
21	6.7 ± 2.1	13.4 ± 1.1
22	40.3 ± 0.5	>300
23	39.9 ± 1.2	>300
24	6.8 ± 3.2	11.9 ± 0.3
25	11.1 ± 2.4	13.0 ± 1.3
26	22.0 ± 0.9	>300
terbinafine hydrochloride (positive control)	0.008 ± 0.373	1.647 ± 0.101

^a Compounds **2**, **4–7**, **9–11**, **13**, **14**, **17**, **20**, and **27–37** were inactive (MIC₅₀ > 300 μM).

3. Experimental Section

3.1. General Experimental Procedures

This part can be found in the Supplementary Materials.

3.2. Plant Material

Whole plants of *G. oppositifolius* were bought from Zay cho market of Mandalay in Myanmar, in December 2015. The plants were identified by author, Jun Yang. A voucher specimen (No. MD1612078) was deposited at the Yunnan Key Laboratory for Wild Plant Resources, Kunming Institute of Botany, Chinese Academy of Sciences.

3.3. Extraction and Isolation

Powdered whole plants of *G. oppositifolius* (3.0 kg) were extracted with 70% EtOH at 60 °C for six times (each for 4 h) to obtain a crude extract (650.1 g), which was suspended in H₂O and then extracted with petroleum ether. The water-soluble phase was adjusted to pH 1–2 with 1% HCl and then partitioned with EtOAc to afford the EtOAc-soluble extract (B, 130.0 g). The aqueous phase was basified with 5% NaOH solution to pH 9–10 and then extracted with CHCl₃ to yield the CHCl₃-soluble extract (A, 25.2 g). The aqueous phase was extracted with *n*-butanol to yield the *n*-butanol-soluble extract (C, 142.0 g).

The CHCl₃ extract (A, 25.2 g) was subjected to silica gel column chromatography (CC, CH₂Cl₂-MeOH, 50:1→0:1, *v/v*) to yield four main fractions A1–A4. Fraction A1 (931.1 mg) was subjected to reversed phase (RP-C₁₈) silica gel CC eluted with MeOH-H₂O (30%→100%). The 30% MeOH-eluted part (86.3 mg) was separated on a Sephadex LH-20 CC (MeOH) and purified by semipreparative HPLC (Welch Ultimate AQ-C₁₈, MeOH-H₂O, 18:82, 0.8 mL/min) to yield **36** (6.0 mg,

$t_R = 56.431$ min). The 60% MeOH-eluted part (399.8 mg) was separated on a Sephadex LH-20 CC (MeOH) to yield **1** (4.9 mg), **2** (4.7 mg), and **31** (24.6 mg) recrystallized from MeOH, as well as **37** (0.4 mg) recrystallized from CH_2Cl_2 . The 80% MeOH-eluted part (127.3 mg) was purified by Sephadex LH-20 CC (CH_2Cl_2 -MeOH, 1:1) and semipreparative HPLC (Agilent Zorbax SB-C₁₈, MeOH-H₂O (containing 0.05% TFA), 67:33, 2 mL/min) to obtain **11** (1.1 mg, $t_R = 36.803$ min) and **9** (5.7 mg, $t_R = 43.850$ min). Fraction A2 (2.1 g) was separated on an RP-18 silica gel CC eluted with MeOH-H₂O (30%→100%). The 70% MeOH-eluted part (96.8 mg) was purified by silica gel CC (CH_2Cl_2 -MeOH-H₂O, 300:10:1) to yield **8** (24.3 mg) recrystallized from MeOH. Fraction A3 (2.5 g) was separated on an RP-18 silica gel CC eluted with MeOH-H₂O (20%→100%). The 60% MeOH-eluted part (965.5 mg) was purified by silica gel CC (EtOAc-MeOH, 20:1) to yield two main subfractions (A3-1 and A3-2). The subfraction A3-1 (91.8 mg) was purified by silica gel CC (CH_2Cl_2 -MeOH, 10:1) and semipreparative HPLC (Agilent Zorbax SB-C₁₈, CH_3CN -H₂O, 35:65, 2 mL/min) to yield **17** (1.0 mg, $t_R = 28.240$ min). The subfraction A3-2 (192.0 mg) was purified by silica gel CC (CH_2Cl_2 -MeOH-H₂O, 80:10:1) to yield two further subfractions (A3-2-1 and A3-2-2). The subfraction A3-2-1 (33.1 mg) was purified by semipreparative HPLC (Agilent Zorbax SB-C₁₈, MeCN-H₂O, 30:70, 2 mL/min) to yield **34** (16.6 mg, $t_R = 31.175$ min) and **16** (7.6 mg, $t_R = 45.162$ min). The subfraction A3-2-2 (7.0 mg) was purified by semipreparative HPLC (Welch Ultimate AQ-C₁₈, MeCN-H₂O, 30:70, 1 mL/min) to yield **35** (1.4 mg, $t_R = 7.176$ min). Fraction A4 (3.0 g) was separated on an RP-C₁₈ silica gel CC eluted with MeOH-H₂O (20%→100%) to yield two further subfractions. The 40% MeOH-eluted part (217.9 mg) was purified by silica gel CC (CH_2Cl_2 -MeOH-H₂O, 70:10:1) to yield **32** (38.4 mg). The 50% MeOH-eluted part (494.4 mg) was recrystallized from MeOH to yield **33** (290.3 mg).

The part of EtOAc extract (B, 27.0 g) was separated on an RP-18 silica gel CC eluted with MeOH-H₂O (5%→100%) to yield five main fractions (B1–B5). The 50% MeOH-eluted part (B1, 2.7 g) was purified by silica gel CC (CH_2Cl_2 -MeOH, 50:1→30:1) to afford **30** (26.8 mg). The 60% MeOH-eluted part (B2, 545.7 mg) was purified by silica gel CC (CH_2Cl_2 -MeOH, 30:1) to yield **12** (5.5 mg). The 70% MeOH-eluted part (B3, 2.5 g) was purified by silica gel CC (CH_2Cl_2 -MeOH, 30:1→20:1) to afford **28** (11.1 mg) and three main subfractions (B3-1–B3-3). Subfraction B3-1 (29.0 mg) was purified by semipreparative HPLC (Agilent Zorbax SB-C₁₈, MeCN-H₂O (containing 0.05% TFA), 47:53, 2 mL/min) and further by semipreparative HPLC (Agilent Zorbax SB-C₁₈, MeOH-H₂O (containing 0.05% TFA), 75:25, 2 mL/min) to yield **13** (3.9 mg, $t_R = 30.891$ min) and **5** (2.1 mg, $t_R = 41.804$ min). Subfraction B3-2 (91.7 mg) was purified by silica gel CC (CH_2Cl_2 -MeOH, 30:1) and semipreparative HPLC (Agilent Zorbax SB-C₁₈, MeCN-H₂O (containing 0.05% TFA), 50:50, 2 mL/min) to yield **7** (5.3 mg, $t_R = 14.414$ min) and **15** (5.3 mg, $t_R = 16.844$ min). Subfraction B3-3 (459.4 mg) was purified by silica gel CC (CH_2Cl_2 -MeOH, 30:1) and semipreparative HPLC (Agilent Zorbax SB-C₁₈, MeCN-H₂O, 45:55, 2 mL/min) to yield **21** (5.7 mg, $t_R = 12.996$ min), **6** (5.9 mg, $t_R = 16.490$ min), and **14** (3.6 mg, $t_R = 17.736$ min). The 80% MeOH-eluted part (B4, 1.1 g) was purified by silica gel CC (CH_2Cl_2 -MeOH, 30:1) to yield two main subfractions (B4-1 and B4-2). Subfraction B4-1 (97.3 mg) was purified by semipreparative HPLC (Agilent Zorbax SB-C₁₈, MeCN-H₂O (containing 0.05% TFA), 45:55, 2 mL/min) to afford **24** (18.3 mg, $t_R = 42.714$ min), **26** (29.0 mg, $t_R = 51.174$ min), and **10** (1.6 mg, $t_R = 62.511$ min). Subfraction B4-2 (153.1 mg) was purified by semipreparative HPLC (Agilent Zorbax SB-C₁₈, MeCN-H₂O (containing 0.05% TFA), 43:57, 2 mL/min) to yield **25** (12.4 mg, $t_R = 37.244$ min), **22** (42.6 mg, $t_R = 45.406$ min), **23** (16.2 mg, $t_R = 66.231$ min), and a mixture. The mixture was purified by semipreparative HPLC (Agilent Eclipse XDB-C₁₈, MeCN-H₂O (containing 0.05% TFA), 40:60, 1 mL/min) to yield **20** (3.5 mg, $t_R = 18.741$ min). The 90% MeOH-eluted part (B5, 1.1 g) was separated on a Sephadex LH-20 CC (MeOH) to yield two main subfractions (B5-1 and B5-2). Subfraction B5-1 (535.3 mg) was purified by silica gel CC (CH_2Cl_2 -MeOH, 30:1) and semipreparative HPLC (Agilent Zorbax SB-C₁₈, MeCN/H₂O (containing 0.05% TFA), 49:51, 2 mL/min) to yield **19** (3.9 mg, $t_R = 43.926$ min). Subfraction B5-2 (244.5 mg) was purified by silica gel CC (petroleum ether-EtOAc, 2:1→1:1) to yield two further subfractions (B5-2-1 and B5-2-2). Subfraction B5-2-1 (52.9 mg) was purified by semipreparative HPLC (Agilent Zorbax SB-C₁₈, MeCN-H₂O (containing 0.05% TFA), 60:40, 2 mL/min) to yield **3** (7.6 mg,

$t_R = 35.867$ min), **4** (3.5 mg, $t_R = 47.842$ min), and **27** (21.0 mg, $t_R = 53.439$ min). Subfraction B5-2-2 (20.2 mg) was purified by semipreparative HPLC (Agilent Zorbax SB-C₁₈, MeCN-H₂O (containing 0.05% TFA), 70:30, 2 mL/min) to yield **29** (0.7 mg, $t_R = 15.194$ min) and **18** (3.1 mg, $t_R = 16.328$ min).

3.4. Spectroscopic and Physical Data

3 β ,12 β ,16 β ,21 β ,22-Pentahydroxyhopane (**1**). Colorless blocks (Me-H₂O, 10:1); $[\alpha]_D^{25} -18$ (*c* 0.05, MeOH); UV (MeOH) λ_{max} (log ϵ) 203 (3.34) nm; ECD (*c* 0.05, MeOH) λ_{max} ($\Delta\epsilon$) 240 (+0.35), 226 (−0.36), 198 (+1.15) nm; ¹H and ¹³C-NMR data, see Table 1; ESIMS *m/z* 515 [M + Na]⁺; HRESIMS *m/z* 515.3718 [M + Na]⁺ (calcd for C₃₀H₅₂NaO₅, 515.3712).

Crystal data for **1**: C₃₀H₅₂O₅, *M* = 524.75, *a* = 7.8358(3) Å, *b* = 17.7389(6) Å, *c* = 20.4841(7) Å, $\alpha = 90^\circ$, $\beta = 90^\circ$, $\gamma = 90^\circ$, *V* = 2847.26(17) Å³, *T* = 100.(2) K, space group *P*212121, *Z* = 4, μ (Cu K α) = 0.653 mm^{−1}, 51,068 reflections measured, 5642 independent reflections (*R*_{int} = 0.0514). The final *R*₁ values were 0.0363 (*I* > 2 σ (*I*)). The final *wR*(*F*²) values were 0.1081 (*I* > 2 σ (*I*)). The final *R*₁ values were 0.0371 (all data). The final *wR*(*F*²) values were 0.1102 (all data). The goodness of fit on *F*² was 0.998. Flack parameter = 0.02(5). The supplementary crystallographic data can be obtained free of charge from the Cambridge Crystallographic Data Centre (CCDC) (deposition number CCDC 1917520) via <http://www.ccdc.cam.ac.uk>.

12 β ,16 β ,21 β ,22-Tetrahydroxyhopan-3-one (**2**). White powder; $[\alpha]_D^{25} +2$ (*c* 0.12, MeOH); UV (MeOH) λ_{max} (log ϵ) 280 (1.98), 219 (2.73), 203 (2.91) nm; ECD (*c* 0.12, MeOH) λ_{max} ($\Delta\epsilon$) 289 nm (+0.17), 232 (+0.28), 208 (−0.29) nm; IR ν_{max} (KBr) 3443, 3427, 1690, 1452, 1385, 1084, 1047, 879 cm^{−1}; ¹H and ¹³C-NMR data, see Table 1; ESIMS *m/z* 513 [M + Na]⁺; HRESIMS *m/z* 513.3551 [M + Na]⁺ (calcd for C₃₀H₅₀NaO₅, 513.3556).

The 3-Oxo-olean-12-ene-28,30-dioic acid (**3**). White powder; $[\alpha]_D^{25} +59$ (*c* 0.26, MeOH); UV (MeOH) λ_{max} (log ϵ) 371 (1.73), 252 (2.75), 239 (2.72) nm; ¹H and ¹³C-NMR data, see Table 2; ESIMS *m/z* 507 [M + Na]⁺; HRESIMS *m/z* 507.3084 [M + Na]⁺ (calcd for C₃₀H₄₄NaO₅, 507.3086).

The 3 β -Hydroxyoleana-11,13(18)-diene-28,29-dioic acid 29-methyl ester (**4**). White powder; $[\alpha]_D^{26} -7$ (*c* 0.15, MeOH); UV (MeOH) λ_{max} (log ϵ) 250 (2.65), 242 (2.59) nm; ECD (*c* 0.09, MeOH) λ_{max} ($\Delta\epsilon$) 250 (−3.92) nm; ¹H and ¹³C-NMR data, see Table 2; ESIMS *m/z* 521 [M + Na]⁺; HRESIMS *m/z* 521.3234 [M + Na]⁺ (calcd for C₃₁H₄₆NaO₅, 521.3237).

Glinusopposide A (**5**). White powder; $[\alpha]_D^{26} -8$ (*c* 0.05, MeOH); ¹H and ¹³C-NMR data, see Table 3; ESIMS *m/z* 613 [M + Na]⁺; HRESIMS: *m/z* 613.4068 [M + Na]⁺ (calcd for C₃₅H₅₈NaO₇, 613.4080).

Glinusopposide B (**6**). White powder; $[\alpha]_D^{25} -20$ (*c* 0.1, MeOH); ¹H and ¹³C-NMR data, see Table 3; ESIMS *m/z* 759 [M + Na]⁺; HRESIMS *m/z* 759.4650 [M + Na]⁺ (calcd for C₄₁H₆₈NaO₁₁, 759.4659).

Glinusopposide C (**7**). White powder; $[\alpha]_D^{26} -6$ (*c* 0.35, MeOH); ¹H and ¹³C-NMR data, see Table 3; ESIMS *m/z* 759 [M + Na]⁺; HRESIMS *m/z* 759.4656 [M + Na]⁺ (calcd for C₄₁H₆₈NaO₁₁, 759.4659).

Glinusopposide D (**8**). White powder; $[\alpha]_D^{21} -36$ (*c* 0.16, pyridine); UV (MeOH) λ_{max} (log ϵ) 275 (2.77), 245 (3.02), 204 (3.59) nm; ECD (*c* 0.099, MeOH) λ_{max} ($\Delta\epsilon$) 284 (+1.00), 249 (−0.17), 218 (+1.03), 197 (−1.11) nm; ¹H and ¹³C-NMR data, see Table 4; ESIMS *m/z* 833 [M + K]⁺, 817 [M + Na]⁺; HRESIMS *m/z* 817.4709 [M + Na]⁺ (calcd for C₄₃H₇₀NaO₁₃, 817.4714).

Glinusopposide E (**9**). White powder; $[\alpha]_D^{20} -32$ (*c* 0.09, MeOH); UV (MeOH) λ_{max} (log ϵ) 415 (2.39), 206 (4.09) nm; ECD (*c* 0.065, MeOH) λ_{max} ($\Delta\epsilon$) 284 (+0.48), 206 (+0.73), 200 (−1.80) nm; IR ν_{max} (KBr) 3442, 3428, 1677, 1644, 1449, 1431, 1385, 1202, 1144, 1086, 1047, 879 cm^{−1}; ¹H and ¹³C-NMR data, see Table 4; ESIMS *m/z* 843 [M + Na]⁺; HRESIMS *m/z* 843.4867 [M + Na]⁺ (calcd for C₄₅H₇₂NaO₁₃, 843.4871).

Glinusopposide F (**10**). White solid; $[\alpha]_D^{25} -31$ (*c* 0.04, MeOH); ¹H and ¹³C-NMR data, see Table 4; ESIMS *m/z* 885 [M + Na]⁺; HRESIMS *m/z* 885.4930 [M + Na]⁺ (calcd for C₄₇H₇₄NaO₁₄, 885.4976).

Glinusopposide G (**11**). White powder; $[\alpha]_D^{20} -7$ (*c* 0.15, MeOH); UV (MeOH) λ_{\max} ($\log \epsilon$) 252 (3.21), 206 (3.81) nm; ECD (*c* 0.078, MeOH) λ_{\max} ($\Delta \epsilon$) 201 (−1.59), 197 (+1.29) nm; IR ν_{\max} (KBr) 3448, 3427, 1639, 1447, 1383, 1084, 1046, 879 cm^{-1} ; ^1H and ^{13}C -NMR data, see Table 4; ESIMS m/z 829 $[\text{M} + \text{Na}]^+$; HRESIMS m/z 829.4711 $[\text{M} + \text{Na}]^+$ (calcd for $\text{C}_{44}\text{H}_{70}\text{NaO}_{13}$, 829.4714).

Glinusopposide H (**12**). White powder; $[\alpha]_D^{25} +7$ (*c* 0.28, MeOH); ^1H and ^{13}C -NMR data, see Table 5; ESIMS m/z 641 $[\text{M} + \text{Na}]^+$; HRESIMS m/z 641.4021 $[\text{M} + \text{Na}]^+$ (calcd for $\text{C}_{36}\text{H}_{58}\text{NaO}_8$, 641.4024).

Glinusopposide I (**13**). White powder; $[\alpha]_D^{25} -10$ (*c* 0.07, MeOH); ^1H and ^{13}C -NMR data, see Table 5; ESIMS m/z 611 $[\text{M} + \text{Na}]^+$; HRESIMS m/z 611.3898 $[\text{M} + \text{Na}]^+$ (calcd for $\text{C}_{35}\text{H}_{56}\text{NaO}_7$, 611.3924).

Glinusopposide J (**14**). White powder; $[\alpha]_D^{25} -22$ (*c* 0.11, MeOH); ^1H and ^{13}C -NMR data, see Table 5; ESIMS: m/z 757 $[\text{M} + \text{Na}]^+$; HRESIMS m/z 757.4486 $[\text{M} + \text{Na}]^+$ (calcd for $\text{C}_{41}\text{H}_{66}\text{NaO}_{11}$, 757.4503).

Glinusopposide K (**15**). White powder; $[\alpha]_D^{25} -16$ (*c* 0.13, MeOH); ^1H and ^{13}C -NMR data, see Table 6; ESIMS m/z 757 $[\text{M} + \text{Na}]^+$; HRESIMS m/z 757.4510 $[\text{M} + \text{Na}]^+$ (calcd for $\text{C}_{41}\text{H}_{66}\text{NaO}_{11}$, 757.4503).

Glinusopposide L (**16**). White powder; $[\alpha]_D^{25} -25$ (*c* 0.1, MeOH); UV (MeOH) λ_{\max} ($\log \epsilon$) 203 (3.82) nm; ECD (*c* 0.076, MeOH) λ_{\max} ($\Delta \epsilon$) 196 (−6.89) nm; IR ν_{\max} (KBr) 3425, 1632, 1454, 1385, 1129, 1094, 1047, 974 cm^{-1} ; ^1H and ^{13}C -NMR data, see Table 6; ESIMS m/z 731 $[\text{M} + \text{Na}]^+$; HRESIMS m/z 731.4353 $[\text{M} + \text{Na}]^+$ (calcd for $\text{C}_{39}\text{H}_{64}\text{NaO}_{11}$, 731.4346).

Glinusopposide M (**17**). White powder; $[\alpha]_D^{20} -25$ (*c* 0.05, MeOH); UV (MeOH) λ_{\max} ($\log \epsilon$) 203 (3.54) nm; ECD (*c* 0.05, MeOH) λ_{\max} ($\Delta \epsilon$) 206 (−4.38), 196 (+4.32) nm; IR ν_{\max} (KBr) 3443, 3426, 1639, 1453, 1421, 1384, 1084, 1047, 879 cm^{-1} ; ^1H and ^{13}C -NMR data, see Table 6; ESIMS m/z 731 $[\text{M} + \text{Na}]^+$; HRESIMS m/z 731.4347 $[\text{M} + \text{Na}]^+$ (calcd for $\text{C}_{39}\text{H}_{64}\text{NaO}_{11}$, 731.4346).

Glinusopposide N (**18**). White powder; $[\alpha]_D^{26} -7$ (*c* 0.18, MeOH); UV (MeOH) λ_{\max} ($\log \epsilon$) 250 (3.76), 213 (3.38) nm; ^1H and ^{13}C -NMR data, see Table 7; ESIMS m/z 567 $[\text{M} + \text{Na}]^+$; HRESIMS m/z 567.3655 $[\text{M} + \text{Na}]^+$ (calcd for $\text{C}_{33}\text{H}_{52}\text{NaO}_6$, 567.3656).

Glinusopposide O (**19**). White powder; $[\alpha]_D^{25} -14$ (*c* 0.13, MeOH); UV (MeOH) λ_{\max} ($\log \epsilon$) 250 (3.76), 218 (3.43) nm; ^1H and ^{13}C -NMR data, see Table 7; ESIMS m/z 729 $[\text{M} + \text{K}]^+$, 713 $[\text{M} + \text{Na}]^+$; HRESIMS m/z 713.4200 $[\text{M} + \text{Na}]^+$ (calcd for $\text{C}_{39}\text{H}_{62}\text{NaO}_{10}$, 713.4241).

Glinusopposide P (**20**). White powder; $[\alpha]_D^{25} -39$ (*c* 0.1, MeOH); UV (MeOH) λ_{\max} ($\log \epsilon$) 250 (4.07), 217 (3.68) nm; ^1H and ^{13}C -NMR data, see Table 7; ESIMS m/z 857 $[\text{M} + \text{Na}]^+$; HRESIMS m/z 857.4300 $[\text{M} + \text{Na}]^+$ (calcd for $\text{C}_{44}\text{H}_{66}\text{NaO}_{15}$, 857.4299).

Glinusopposide Q (**21**). White powder; $[\alpha]_D^{25} +40$ (*c* 0.13, MeOH); ^1H and ^{13}C -NMR data, see Table 8; ESIMS m/z 726 $[\text{M} + \text{Na}]^+$; HRESIMS m/z 726.4201 $[\text{M} + \text{Na}]^+$ (calcd for $\text{C}_{39}\text{H}_{61}\text{NNaO}_{10}$, 726.4193).

Glinusopposide R (**22**). White powder; $[\alpha]_D^{25} +10$ (*c* 0.15, MeOH); ECD (*c* 0.078, MeOH) λ_{\max} ($\Delta \epsilon$) 221 (−1.44) nm; ^1H and ^{13}C -NMR data, see Table 8; ESIMS m/z 859 $[\text{M} + \text{Na}]^+$; HRESIMS m/z 859.4452 $[\text{M} + \text{Na}]^+$ (calcd for $\text{C}_{44}\text{H}_{68}\text{NaO}_{15}$, 859.4450).

Glinusopposide S (**23**). White powder; $[\alpha]_D^{25} +8$ (*c* 0.1, MeOH); ^1H and ^{13}C -NMR data, see Table 8; ESIMS m/z 873 $[\text{M} + \text{Na}]^+$; HRESIMS m/z 873.4606 $[\text{M} + \text{Na}]^+$ (calcd for $\text{C}_{45}\text{H}_{70}\text{NaO}_{15}$, 873.4607).

Glinusopposide T (**24**). White powder; $[\alpha]_D^{24} +71$ (*c* 0.22, MeOH); ^1H and ^{13}C -NMR data, see Table 9; ESIMS m/z 655 $[\text{M} + \text{Na}]^+$; HRESIMS m/z 655.3820 $[\text{M} + \text{Na}]^+$ (calcd for $\text{C}_{36}\text{H}_{56}\text{NaO}_9$, 655.3822).

Glinusopposide U (**25**). White powder; $[\alpha]_D^{25} +11$ (*c* 0.1, MeOH); ^1H and ^{13}C -NMR data, see Table 9; ESIMS m/z 801 $[\text{M} + \text{Na}]^+$; HRESIMS m/z 801.4393 $[\text{M} + \text{Na}]^+$ (calcd for $\text{C}_{42}\text{H}_{66}\text{NaO}_{13}$, 801.4396).

The 3 β -O-(6-O-Methyl- β -D-glucuronopyranosyl)-olean-12-ene-28,30-dioic acid 30-methyl ester (**26**). White powder; $[\alpha]_D^{25} +66$ (*c* 0.12, MeOH); ^1H and ^{13}C -NMR data, see Table 9; ESIMS m/z 713 $[\text{M} + \text{Na}]^+$; HRESIMS m/z 713.3871 $[\text{M} + \text{Na}]^+$ (calcd for $\text{C}_{38}\text{H}_{58}\text{NaO}_{11}$, 713.3877).

3.5. Acid Hydrolysis and Sugar Analysis

3.5.1. Acid Hydrolysis of **31** and Acetylation of Xylose

Compound **31** (15.5 mg) was dissolved in 2 M HCl (1 mL) and stirred at 90 °C for 4 h. After cooling, the solution was evaporated to dryness under reduced pressure. The reaction mixture was purified by silica gel column chromatography (CH₂Cl₂-MeOH-H₂O, 500:10:1, 300:10:1, 200:10:1) to afford xylose (1.9 mg). The sugar was dissolved in pyridine (0.1 mL) and acetic anhydride (0.1 mL) and stirred for 21 h at room temperature. Then, water (5 mL) was added to the reaction mixture, followed by extraction with EtOAc (5 mL). The organic layer was dried under reduced pressure to yield 1,2,3,4-tetra-*O*-acetyl-*D*-xylopyranose (0.9 mg), which was identified based on its ¹H-NMR spectrum and optical rotation value: $[\alpha]_D^{21} -31$ (c 0.08, CHCl₃) [21].

3.5.2. Acid Hydrolysis of the Saponin Mixture and Acetylation of Rhamnose

The *n*-butanol-soluble part (20.0 g) was subjected to D101 resin column chromatography, eluted using water (discarded) and 60% EtOH to yield the saponin mixture (4.0 g). The latter (1.0 g) was dissolved in 2 M HCl (3 mL) and stirred at 90 °C for 5 h. The reaction mixture was dried and purified by silica gel column chromatography (CH₂Cl₂-MeOH-H₂O, 500:10:1, 200:10:1, 100:10:1) to yield rhamnose (97.9 mg) and glucose (9.4 mg). The glucose was identified as *D*-glucose based on its ¹H-NMR spectrum and optical rotation value: $[\alpha]_D^{19} +40$ (c 0.22, H₂O) [22]. The rhamnose (97.9 mg) was dissolved in pyridine (0.1 mL) and acetic anhydride (0.1 mL) and stirred for 21 h at room temperature. Then, water (5 mL) was added to the reaction mixture, followed by extraction with EtOAc (5 mL). The organic layer was dried under reduced pressure and purified by silica gel column chromatography (petroleum ether-EtOAc, 50:1) to yield 1,2,3,4-tetra-*O*-acetyl- α -*L*-rhamnopyranose (1.4 mg), which was identified based on its ¹H-NMR spectrum and optical rotation value: $[\alpha]_D^{21} -27$ (c 0.14, CHCl₃) [23].

3.6. Antimicrobial Assays

The fungi strains *T. rubrum* ATCC 4438 and *M. gypseum* CBS118893) were purchased from the Institute of Dermatology and Hospital for Skin Diseases, Chinese Academy of Medical Sciences. An antifungal assay was performed according to modified versions of the clinical and laboratory standards institute (CLSI), formerly national committee for clinical laboratory standards (NCCLS) methods, as described previously [24,25]. Terbinafine hydrochloride was used as a positive control. The 50% minimum inhibitory concentration (MIC₅₀) was calculated by the Reed-Muench method [26].

4. Conclusions

In this study, four new triterpenoids (**1–4**), 21 new triterpenoids glycosides (**5–25**), and 12 known compounds were isolated from *G. oppositifolius*. However, we cannot exclude the possibility that some of the isolated compounds might be artifacts resulted from the extraction treatment, for example compound **23** might be artifacts of ethanol extraction. The triterpenoids and their glycosides were hopane-type and oleanane-type which have been proofed to be existing in this plant [9,13]. Four compounds including glinusopposide B (**6**), glinusopposide Q (**21**), glinusopposide T (**24**), and glinusopposide U (**25**) showed considerable inhibitory activities against *M. gypseum* and *T. rubrum*. According to the study of SARs, sugars at 3-hydroxy, 30-carboxymethyl group, and the double bond at C-12 play a key role in oleanane type compounds for antifungal activities. The SARs of hopane type compounds for antifungal activities remain for further research. This study provides a scientific evidence of traditional practice on applying *G. oppositifolius* to treat dermatophytosis.

Supplementary Materials: The following are available online. General experimental procedures; Figures S1–S198: 1D and 2D-NMR and HRESIMS spectra of compounds **1–26**, structures of known compounds (**26–37**), and key 2D-NMR correlations of **2**, **6–11**, and **13–25**.

Author Contributions: Y.W. and X.Y. designed the research; D.Z. performed the research; J.Y. identified the plant of study; M.M.S. and T.N.O. provided the material and traditional knowledge; D.Z. and Y.W. analyzed the data and wrote the paper. Y.W., X.Y., and Y.F. revised the manuscript. X.-N.L. provided the data of single-crystal X-ray diffraction. All authors have read and approved the final manuscript.

Funding: This study was supported by the Southeast Asia Biodiversity Research Institute, Chinese Academy of Sciences (no. 2015CASEABRIRG001 and Y4ZK111B01), the National Natural Science Foundation of China (no. 31670338), and the International Partnership Program of Chinese Academy of Sciences (no. 153631KYSB20160004).

Acknowledgments: We thank to Xue Bai, at Kunming Institute of Botany, Chinese Academy of Sciences, for the antifungal assay.

Conflicts of Interest: The authors declare no conflict of interest.

References

1. Abd Elmegeed, A.S.M.; Ouf, S.A.; Moussa, T.A.A.; Eltahlawi, S.M.R. Dermatophytes and other associated fungi in patients attending to some hospitals in Egypt. *Braz. J. Microbiol.* **2015**, *46*, 799–805. [[CrossRef](#)] [[PubMed](#)]
2. Silva, K.V.S.; Lima, M.I.O.; Cardoso, G.N.; Santos, A.S.; Silva, G.S.; Pereira, F.O. Inhibitory effects of linalool on fungal pathogenicity of clinical isolates of *Microsporium canis* and *Microsporium gypseum*. *Mycoses* **2017**, *60*, 387–393. [[CrossRef](#)] [[PubMed](#)]
3. Lu, D.; Hartmann, H.E.K. Molluginaceae. In *Flora of China*; Wu, Z.Y., Raven, P.H., Hong, D.Y., Eds.; Science Press: Beijing, China; Missouri Botanical Garden Press: St. Louis, MO, USA, 2003; Volume 5, pp. 437–439.
4. Sheu, S.Y.; Yao, C.H.; Lei, Y.C.; Kuo, T.F. Recent progress in *Glinus oppositifolius* research. *Pharm. Biol.* **2014**, *52*, 1079–1084. [[CrossRef](#)] [[PubMed](#)]
5. Ashin Nargathaynar Biwantha. *Ashin Nargathaynar: Pohn-pya-say-abidan (Illustrated dictionary of traditional Medicinal plants) (Myanmar version)*; Mingalar Press: Yangon, Myanmar, 1971; Volume 5, pp. 57–58.
6. Editorial Board of “*Zhonghua Bencao*”, State Administration of Traditional Chinese Medicine of the People’s Republic of China. *Zhonghua Bencao*; Shanghai Scientific and Technical Publishers: Shanghai, China, 1999; Volume 2, pp. 751–752.
7. Hariharan, V.; Rangaswami, S. Steroids and triterpenoids from the roots of *Mollugo spergula*. *Phytochemistry* **1971**, *10*, 621–624. [[CrossRef](#)]
8. Kumar, D.; Shah, V.; Ghosh, R.; Pal, B.C. A new triterpenoid saponin from *Glinus oppositifolius* with α -glucosidase inhibitory activity. *Nat. Prod. Res.* **2013**, *27*, 624–630. [[CrossRef](#)] [[PubMed](#)]
9. Ragasa, C.Y.; Cabrera, E.C.; Torres, O.B.; Buluran, A.I.; Espineli, D.L.; Raga, D.D.; Shen, C.C. Chemical constituents and bioactivities of *Glinus oppositifolius*. *Pharmacognosy Res.* **2015**, *7*, 138–147. [[CrossRef](#)] [[PubMed](#)]
10. Traore, F.; Faure, R.; Ollivier, E.; Gasquet, M.; Azas, N.; Debrauwer, L.; Keita, A.; Timon-David, P.; Balansard, G. Structure and antiprotozoal activity of triterpenoid saponins from *Glinus oppositifolius*. *Planta Med.* **2000**, *66*, 368–371. [[CrossRef](#)]
11. Zhu, Y.Y.; Qian, L.W.; Zhang, J.; Liu, J.H.; Yu, B.Y. New approaches to the structural modification of olean-type pentacyclic triterpenes via microbial oxidation and glycosylation. *Tetrahedron* **2011**, *67*, 4206–4211. [[CrossRef](#)]
12. Mizui, F.; Kasai, R.; Ohtani, K.; Tanaka, O. Saponins from bran of quinoa, *Chenopodium quinoa* Willd. II. *Chem. Pharm. Bull.* **1990**, *38*, 375–377. [[CrossRef](#)]
13. Sahu, N.P.; Koike, K.; Banerjee, S.; Achari, B.; Nikaido, T. Triterpenoid saponins from *Mollugo spergula*. *Phytochemistry* **2001**, *58*, 1177–1182. [[CrossRef](#)]
14. Tanaka, N.; Yamauchi, K.; Murakami, T.; Saiki, Y.; Chen, C.M. Chemical and chemotactic investigations of filicales. 38. Chemical investigations of the substances contained in *Diplazium subsinuatum* (Wall) Tagawa. *Chem. Pharm. Bull. (Tokyo)* **1982**, *30*, 3632–3639. [[CrossRef](#)]
15. Kim, K.H.; Lee, I.K.; Choi, S.U.; Lee, J.H.; Moon, E.; Kim, S.Y.; Lee, K.R. New triterpenoids from the tubers of *Corydalis ternata*: Structural elucidation and bioactivity evaluation. *Planta Med.* **2011**, *77*, 1555–1558. [[CrossRef](#)] [[PubMed](#)]
16. Awanchiri, S.S.; Trinh-Van-Dufat, H.; Shirri, J.C.; Dongfack, M.D.J.; Nguenang, G.M.; Boutefnouchet, S.; Fomum, Z.T.; Seguin, E.; Verite, P.; Tillequin, F.; et al. Triterpenoids with antimicrobial activity from *Drypetes inaequalis*. *Phytochemistry* **2009**, *70*, 419–423. [[CrossRef](#)] [[PubMed](#)]

17. Melek, F.R.; Miyase, T.; El-Gindi, O.D.; Abdel-Khalik, S.M.; Haggag, M.Y. Saponins from *Fagonia mollis*. *Phytochemistry* **1996**, *42*, 1405–1407. [[CrossRef](#)]
18. Ragasa, C.Y.; Espineli, D.L.; Mandia, E.H.; Don, M.J.; Shen, C.C. A new triterpene from *Glinus oppositifolius*. *Chin. J. Nat. Medicines* **2012**, *10*, 284–286. [[CrossRef](#)]
19. Kuang, H.X.; Yang, B.Y.; Xia, Y.G.; Feng, W.S. Chemical constituents from the flower of *Datura metel* L. *Arch. Pharm. Res.* **2008**, *31*, 1094–1097. [[CrossRef](#)]
20. Corbally, R.P.; Mehta, L.K.; Parrick, J.; Short, E.L. Experimental and calculated ^{13}C chemical shifts for α -, β -, γ - and δ -carbolines. *Magn. Reson. Chem.* **2000**, *38*, 1034–1036. [[CrossRef](#)]
21. Šardžik, R.; Noble, G.T.; Weissenborn, M.J.; Martin, A.; Webb, S.J.; Flitsch, S.L. Preparation of aminoethyl glycosides for glycoconjugation. *Beilstein J. Org. Chem.* **2010**, *6*, 699–703. [[CrossRef](#)]
22. Wang, Y.H.; Wang, J.H.; He, H.P.; Zhou, H.; Yang, X.W.; Li, C.S.; Hao, X.J. Norsesquiterpenoid glucosides and a rhamnoside of pyrrolizidine alkaloid from *Tephrosia kirilowii*. *J. Asian Nat. Prod. Res.* **2008**, *10*, 25–31. [[CrossRef](#)]
23. Li, E.W.; Gao, X.; Gao, K.; Jia, Z.J. Labdane diterpenoid glycosides from *Aster veitchianus*. *Chem. Biodivers.* **2007**, *4*, 531–538. [[CrossRef](#)]
24. National Committee on Clinical Laboratory Standards (NCCLS). *Reference Method for Broth Dilution Antifungal Susceptibility Testing of Yeasts*; Approved standard NCCLS document M27-A2; National Committee on Clinical Laboratory Standards: Wayne, PA, USA, 2002.
25. Clinical and Laboratory Standards Institute (CLSI). *Methods for Dilution Antimicrobial Susceptibility Tests for Bacteria That Grow Aerobically*; Approved standard, M7-A7; Clinical and Laboratory Standards Institute: Wayne, PA, USA, 2006.
26. Reed, L.J.; Muench, H. A simple method of estimating fifty percent end points. *Am. J. Hyg.* **1938**, *27*, 493–497.

Sample Availability: Samples of the compounds **8**, **31**, **33**, and **34** are available from the authors.



© 2019 by the authors. Licensee MDPI, Basel, Switzerland. This article is an open access article distributed under the terms and conditions of the Creative Commons Attribution (CC BY) license (<http://creativecommons.org/licenses/by/4.0/>).